7LS1M0: Masterproject BPS A Research

The Fire Resilience of CLT Compartments in comparison to Non-Flammable Compartments

Semester A - 2025-2026

Full Name	Student ID
H.D.S. van Dongen	1836757

Architecture, Building and Planning
Building Physics and Services department

Supervisor: ir. R.A.P. van Herpen FIFireE

Eindhoven, February 9, 2026

1 Abstract

In light of sustainability, renewable materials such as cross-laminated timber (CLT) are increasingly applied in the built environment. However, due to their flammable characteristics, these materials influence fire dynamics differently than traditional non-combustible building materials. Since the objective of employing these materials is based on sustainability, building design should also reflect this by addressing not only fire safety but also fire resilience. However, the concept of fire resilience is inadequately addressed in current building regulations. Additionally, while research on the fire behaviour of CLT has expanded and numerous experimental studies have been conducted, simulation-based studies remain limited due to the high level of assumptions and uncertainty.

This study investigates how fire behaviour and fire resilience within CLT compartments can be determined through iterative simulations using the natural fire concept. Different scenarios with varying degrees of exposed and protected CLT surfaces were analysed and compared on the effects of fire resilience. The results indicate that compartments with a singular exposed CLT surface tend to self-extinct, whereas compartments with multiple exposed CLT surfaces generally exhibit a burn-down scenario. These insights suggest that a fire-resilient design can be achieved by limiting exposed CLT surfaces and applying adequate fire protection to other surfaces. This approach not only enhances occupant safety but also contributes to a more sustainable and durable application of the materials.

2 Nomenclature

Parameter	Unit	Definition
A_f	m^2	Area of the floor of the compartment
A_i	m^2	Area of exposed surfaces
b_p	m	Width of the radiation panel
b_s	m	Width of the CLT sample
c_v	J/kgK	Specific heat of air at constant volume
d_i	m	Thickness of the exposed surface
e		Emission-absorption coefficient
E	J	Energy in the compartment due to the fire
f_{tot}		Total view-factor
H	MJ/kg	Caloric value
h_p	m	Height of the radiation panel
h_s	m	Height of the CLT sample
$m_{l,A,avg}$	kg/m^2	Average mass loss per m^2 of sample for full time duration
m_{ox}	kg	Oxygen mass in the compartment
p_{burned}	MJ	Burned permanent fire load
p_{perm}	MJ/m^2	Permanent fire load of the compartment
$p_{remaining}$	MJ	Remaining permanent fire load of the compartment
q_r	kW/m^2	Received radiation flux
q_{source}	kW/m^2	Radiation flux of the source
ρ	kg/m^3	Density
RHR_c	kW/m^2	Transformed rate of heat release for the compartment
RHR_s	kW/m^2	Produced rate of heat release in experiments by Van Poppel
σ	W/m^2K^4	Stefan Boltzmann constant
t	s	Time duration
t_{burned}	s	Time duration for all permanent fire load to be burned
$t_{<T_{min}}$	s	The point in time where the gas temperature is below the minimum value of the temperature interval
τ		Transmission coefficient
T_a	K	Ambient temperature
T_r	K	Radiative gas temperature

Contents

3 Introduction

Over the past decades, the demand for sustainable construction materials in the built environment has increased significantly. As non-renewable resources are gradually exhausted, reducing dependency on these materials has become increasingly important. In addition, renewable materials typically result in lower greenhouse gas emissions than non-renewable materials, so the application of renewable materials is also preferable for reducing global emissions as determined by the Paris Agreement. Timber is a reputable renewable building material, which is also increasingly employed as cross-laminated timber (CLT). [17] CLT, compared to traditional construction materials, is a combustible material, and can add significantly to a fire [24]. Although CLT is a renewable material, when burning it releases a significant amount of greenhouse gas emissions, which is unfavourable from a sustainability perspective. Furthermore, CLT can exhibit a burn-down scenario, implying that the entire structure needs to be demolished and rebuilt, causing the demand for a considerable amount of resources. By ensuring the fire resilience of a building, occupants, other properties and the structure itself are protected, reducing both emissions and resource demands, aiding to the sustainability aspect of renewable materials.

3.1 Problem Definition

Despite these developments, building codes concentrate on fire safety, while the concept of fire resilience is underrepresented. With the significant increase in the application of CLT, research interest is spreading. Numerous experimental studies have been performed on the behaviour of CLT in a compartment fire, however these experiments use a large amount of resources and result in high levels of emissions. Simulations, which allow for testing an infinite number of scenarios with minimal resources, however, are not often used due to the high level of assumptions and uncertainty. The aim of this research is to determine the fire resilience of different scenarios of a CLT compartment with surface protection, using iterative simulations in the OZone simulation software with a natural fire concept. Furthermore, the goal is to determine what level of surface protection is required in order to ensure fire-resilience. These objectives are translated in the main research question:

> *"How does the fire resilience of a CLT compartment differ from a non-flammable compartment under simulated natural fire conditions, and how can fire-resistant materials improve the fire performance of the CLT compartment?"*

This research question is further supported by the following questions:

- What influences the fire dynamics in a CLT compartment, as determined through literature?
- Using iterative simulation in OZone, how do fire dynamics, such as the temperature evolution and heat release rate, differ between scenarios?
- How does the fire protection of CLT surfaces influence the fire dynamics and fire resilience in CLT compartments?
- What recommendations for fire-safe and resilient design and material selection, such as the required level of fire protection, in CLT construction can be drawn from the simulation results?

3.2 Scope and Limitations

The scope and limitations of this study define the boundaries within which the results should be interpreted. The study focuses on an individual compartment with multiple scenarios regarding exposed and protected CLT surfaces. The compartment has a rectangular configuration and does not include interior divisions. The simulations are performed under the natural fire concept, and the input parameters will be based on the standardised values as determined in building regulations and guidelines in the Netherlands, such as NEN 6055:2009 (natural fire concept) and NEN-EN 1991-1-2+NA (Eurocode 1), at the time of research [21, 37]. This means that no project-specific data is used.

In the simulations, a worst-case scenario is assumed, implying that it is ensured that a lack of oxygen does not limit the rate of heat release of the fire in the simulation. This is achieved by maximising the openings

in the compartment to the size required for sufficient oxygen availability in variable load conditions. Active fire protection measures, such as sprinklers or manual fire suppression methods, are not included to assess the full intensity of the fire. Simulations are continued until the fire self-extinguishes.

3.3 Reading guide

This report is starts with a literature review, in Chapter 4, to establish an understanding of relevant concepts, material properties and behaviour, the theory behind the simulations, and existing experimental studies. This is succeeded by the methodology used in the calculation and simulation of the different scenarios, as discussed in Chapter 5. The results of these calculations and simulations are then discussed in the results in Chapter 6. The interpretation of the results, limitations and possible further research aspects are defined in the discussion in Chapter 7. Finally, the key findings of the study are determined and concluded in Chapter 8.

4 Literature Review

The building sector accounts for a large fraction of global greenhouse gas emissions and energy use. Materials such as brick, steel and concrete require excessive heating processes and material handling, contributing to high emissions and energy usage. Since sustainability has become a more important topic over the years, the material application and construction processes in the built environment have adapted to reduce their impact on the environment. For example, an increasing effort is made to adjust the use of materials with a high level of climatic impact to materials with a low level of climatic impact. This is characterised by an increasing use of timber-based construction materials. Throughout its lifetime, timber stores carbon until it is burned. [24] Accordingly, timber is regarded as a material with low climatic impact, since the manufacturing of the material does not require carbon.

This chapter will elaborate on the existing requirements surrounding structural fire design and the contrast between the concepts of fire safety and fire resilience. Furthermore, a short history of the use of timber as a building material will be provided, as well as a deep dive into cross-laminated timber (CLT) and protective materials. Subsequently, the theory behind the simulation software of OZone used for structural fire design, and the standard parameters utilised in these simulations, are explored. This literature review provides an overview of the theory behind the research objective and the basis for the simulations.

4.1 Fire Safety and Fire Resilience

In the national regulations regarding fire, the concept of "fire safety" is often referred to. Fire safety regulations are mainly focused on the safety of the occupants and the rescue units, as well as the prevention of destruction of other properties [32, 33, 34]. To ensure this, several aspects, such as prevention of ignition, safe exits, prevention of structural collapse and prevention of fire spreading, are implemented in the regulations [33, 36]. The concept of "fire safety", however, does not determine whether or not a building should remain standing after a fire. Thus, "fire safety" can imply that, as long as occupants, rescue units and other properties are protected, the building is allowed to burn down completely. The concept of "fire resilience", on the other hand, refers to a restorable building post-fire. Implying that only minimal restoration is required, without demolition and reconstruction, for a functional fire-resilient building [18]. Thus, aside from considering the safety of occupants, rescue units and surrounding properties, the concept of "fire resilience" also regulates the protection of the building itself from full destruction through fire. Overall, a traditional building constructed from bricks or concrete can pass as fire-resilient, since the load-bearing structure itself does not combust. Regarding a traditional building, only the interior and exterior finishings, insulation and the furniture burn. With minimal renovations, the building structure could be used post-fire. However, in light of sustainability, more housing is constructed out of bio-based materials, such as timber. Unlike the traditional non-flammable materials, timber is susceptible to fire, so buildings with a timber structure will also have a burning structure, aside from the finishings, insulation and furniture. Without proper protection, the building will fully burn and be unrecoverable post-fire, which means that it is not fire resilient.

In the building regulations, several factors regarding fire safety are discussed. Predominantly, the structural safety of a building should be considered. The construction should be able to be resistant to fire, to the extent that it does not cause danger for people evacuating or aiding in evacuation, for a certain period of time [33]. Additionally, the Dutch Building Code states that the occurrence of a fire-hazardous situation should be limited, for example, by considering that materials near a fireplace have a low level of flammability [36]. Also, the development of fire and smoke, in spaces and properties, is to be limited with the materials used inside and outside the building [34], [35].

4.2 Timber as a Building Material

Timber grows through the process photosynthesis, where carbon dioxide (CO_2) from the air and water (H_2O) from the ground are converted to glucose ($C_6H_{12}O_6$) and oxygen (O_2), using the chemical energy originating from sunlight. The glucose molecules bind together in cellulose chains, which, together with hemicellulose and lignin, compose the structure of timber. The cellulose is responsible for the tensile strength of the timber, whereas hemicellulose and lignin are accountable for the compressive strength of the timber. There are many different species of trees, but woods are either hardwoods or softwoods. Hardwoods originate from slow-growing, broad-leafed trees, commonly known as deciduous trees. On the other hand, softwoods originate

from fast-growing, needle-shaped-leafed trees, commonly known as conifers. Hardwoods typically have a more complex microstructure compared to softwoods, following the difference in growing pace. [15, 26] In both types of wood, the trunk of the tree consists of a pith, heartwood and sapwood. The pith is the centre of the tree, around which the new cells grow. This is enveloped by a layer of heartwood, which consists of the dead cells of the tree, providing the tree with structural strength. The sapwood is the outermost layer, consisting of living cells able to transport water, minerals and sugars. [15, 25, 26] Overall, hardwood, due to its larger layer of heartwood owing to its slower growing process, has a higher level of durability, signifying that it is less susceptible to deterioration resulting from weathering, fungi and insects [25, 26].

Timber has already been applied in building structures for aeons, employing many different methods depending on the location, time and locally available raw materials. For example, in the Neolithic Age in China, branches and thatch were used in order to build structures similar to nests on top of a dug-in pit or poles [41]. Likewise, massive timber construction in the form of the Blockbau system, entailing the stacking of (sawn) logs, was widely utilised throughout Europe, where there were a lot of woodlands able to provide sufficient raw materials for this building type [52]. Aside from the massive timber structures, timber skeleton structures were used, for instance, in Amsterdam after the city fire in 1452 [46]. Timber also functions as an addition in structures of roofs and ceilings in stone and brick structures [43]. The application of timber in building structures, especially when buildings are placed in close proximity, also brought about the risk of large and easily spreading fires. One of multiple well-known examples of the combustion risk of timber structures is the Great Fire of London of 1666. The fire started in a bakery in the heart of London, and with a combination of a long, hot and dry summer, strong winds, buildings constructed predominantly out of timber and the proximity of all the buildings to each other, the fire quickly spread throughout the entire city, destroying homes, churches, and more. [7] Another example is the Chicago Fire of 1871, where a fire, which started in a barn, spread throughout the city, again influenced by the dry summer and strong winds [40]. A more recent example is the burning of Notre Dame in Paris, where a spark, resulting from construction work, resulted in a rapid fire spread through the wooden interior of the church, resulting in a collapse of the roof and spire [6]. These large fires demonstrate that, when implementing timber into a building structure, it is important that it is adequately protected and that the risk of fire spreading is limited in order to limit the damage.

According to literature [25, 27, 38], burning timber goes through several stages, depending on the temperatures reached. Initially, the free water in the timber evaporates, by temperatures above the boiling point of water, 100 °C, drying out the timber. Between 160 and 200 °C, polymers such as hemicellulose start to decompose. This is followed by the dehydration of the timber and a slow pyrolysis, between temperatures of 200 to 220 °C. With temperatures between 225 and 275 °C, pyrolysis, the thermal decomposition of the timber through a change in chemical composition and physical phase, is initiated, which then turns into rapid pyrolysis when temperatures exceed 300 °C. Finally, for temperatures above 350 °C, the char continues to smoulder and oxidise. The char, as a result of its reduced conductive heat transfer, forms a protective layer for the still untouched timber on the other side of the fire exposure. However, when oxidising, the timber releases energy, only contributing to further burning of the timber and surrounding surfaces. The exact temperature intervals for the different stages can differ because of variations in the moisture and microstructure of the timber.

4.3 Cross Laminated Timber

There are numerous forms of timber products, in addition to traditional sawn timber directly from the logs, that are used in building construction. These forms can be divided into three groups: particleboards, fibreboards and layered products [15]. Particleboards, such as wood particleboard, cement-bonded particleboard and oriented strand board (OSB), consist of particles of wood, adhesive, and possibly an additive such as cement. The mixture of these particles is pressed into a panel with high pressure and heat. Fibreboards consist of timber fibres, which are smaller particles compared to the ones used in particleboards, and adhesive. Similar to the particleboards, this mixture is pressed together under high pressure and heat to form a panel. Layered products, such as glue-laminated timber (glulam), cross-laminated timber (CLT) and plywood, consist of multiple layers of timber which are stacked and glued to each other using resin or other types of adhesives.[15, 26]

This study will mainly focus on CLT, as prefabricated wall and floor slabs, mainly used in residential

buildings, where they function both as separation constructions and load-bearing structures. CLT is a modern construction material developed in the early 1990's, consisting of multiple large solid timber panels, glued and pressed together perpendicularly [1, 13, 51]. This manufacturing method generates a strong material, which can be used for load-bearing structures, such as walls, floors and roofs. Aside from its structural properties, CLT is also frequently used for its aesthetic in construction, since the surfaces of the load-bearing construction can be left bare. Currently, CLT is generally used in lower (multi-storey) dwellings, with an increasing application in larger-scale projects over time. Overall, research exhibits that the use of CLT in construction saves on average 40% in greenhouse gas emissions compared to traditional building materials for similar building types [51]. Nevertheless, it is ever so important to consider the bio-based nature of the material, which can perform differently from traditional building materials with regard to the moisture, durability, fire, acoustics and energy aspects. Generally, the timber in CLT is a softwood, with a lower level of durability compared to hardwood [1, 24]. Respectively, the CLT should be protected from moisture, and the moisture conditions in the wood should be thoroughly managed in order to prevent the degradation of the building structure. During the production of CLT, several types of adhesives can be used. It is essential that the adhesive bonds well with the timber to guarantee a good-quality structural material. Commonly employed types of adhesives in CLT include polyurethane or formaldehyde-based adhesives [1]. Research shows that formaldehyde-based adhesives generate the highest bonding strength and also perform best when exposed to moisture or increased temperatures. These types of adhesives, however, are more toxic as a result of their volatile organic compound (VOC) release, influencing the occupant's health. Besides the properties of the adhesives themselves, the bonding strength can also be influenced by the adhesive spreading rate and the clamp pressure on the timber boards during the curing process. [1, 38] The material properties of the CLT itself are strongly dependent on the combination between the type(s) of timber, the type of adhesive and the moisture content of the CLT [50].

When exploring the performance of CLT in the instance of fire, it is essential to consider that CLT is a flammable material. Which means that without any fire-resistant protection, a CLT construction will burn along with the variable fire load in the building. A brickwork or concrete structure will remain intact, whereas the structure of a CLT-based building will give out in time. Subsequently, providing additional danger of collapse along with the dangers surrounding the fire itself. Since the structure of a CLT building can burn along with the variable load, the total fire load is significantly larger compared to that of a traditional compartment. The increased fire load contributes to higher gas temperatures and an extended fire duration. The layered nature of CLT creates a risk of heat-induced delamination or char fall-off, as illustrated in Figure 1.

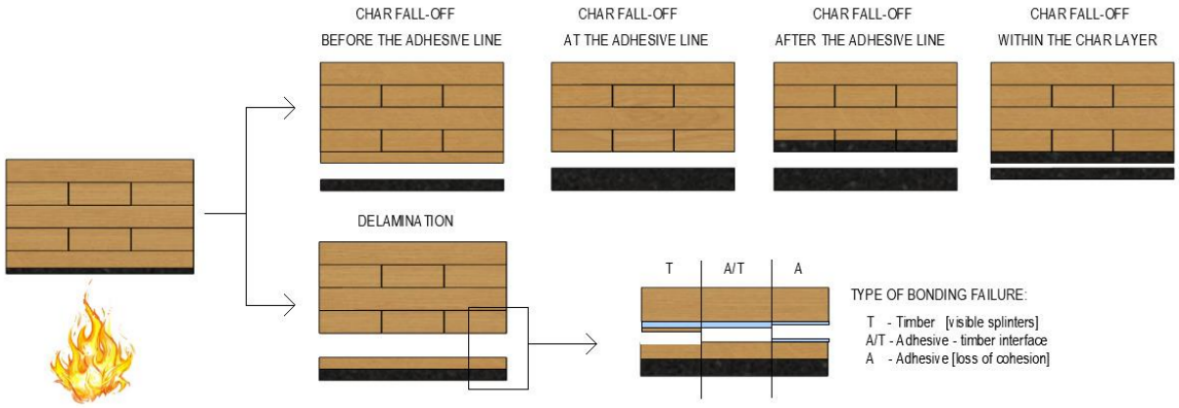

Figure 1: Failure of CLT in the form of char fall-off and delamination [12]

Heat-induced delamination occurs as a result of failure of the adhesive or the bond between the adhesive and the timber. When this happens, fresh timber is exposed to the fire, supplying more fuel to the fire, thus delaying the process of self-extinction. Research suggests that the risk of heat-induced delamination as a result of adhesive failure is strongly related to the type of adhesive, which also emerged in previously

discussed literature, indicating an increased resistance of formaldehyde-based adhesives to extreme heat exposure. Char fall-off is a factor which occurs when completely charred timber pieces detach from the solid timber, exposing fresh timber fuel, similar to heat-induced delamination. Char fall-off can only take place when the temperatures allow for the process of pyrolysis. [24, 38, 44] Both heat-induced delamination and char fall-off can cause a secondary flashover when fresh timber is introduced at the right moment [38]. Additionally to the fresh timber exposed through char fall-off, the oxidation of the char significantly adds to the heat release of burning timber, which can prolong the burning of the timber [27]. Research shows it is complex to determine whether or not a fire in a CLT compartment will self-extinguish, and that the fire needs to comply with several conditions to achieve self-extinguishment, which can again be affected by heat-induced delamination or char fall-off [4, 13, 16, 38].

4.4 Fire Protection

While the use of CLT for construction in itself is a sustainable option, it is important to consider that in the instance of a fire, the construction, without proper fire protection, will inevitably burn along with the variable load. So the stored carbon will be released again. Furthermore, when the CLT structure is burning, the mechanical properties of the material significantly reduce. Possibly resulting in the need for demolition and complete reconstruction if the structure cannot be reused after a fire. A timber construction can be fire resistant according to the standard fire curve, when the reduced cross-section is sufficient to meet the requirements of a separating structure and a load-bearing structure. Here it is assumed that the structure does not burn after a set time duration. However, in a natural fire concept, the burning does not stop, and the CLT structure continues to burn. [44]

The national regulations state a minimum fire resistance of the structure in a range of 30 to 120 minutes, depending on the maximum floor height [31]. For the purpose of determining the fire resilience of the building, the maximum requirement of 120 minutes for the fire resistance is assumed. Gypsum boards are regularly used in the protection of load-bearing structures for their fire-resistant properties. The fire resistance of the gypsum boards follows from the dehydration of the gypsum, which requires significant energy due to its endothermic nature. It is only after the dehydration process is complete that heat transfer occurs through the gypsum boards. [20] The thicker the gypsum board layer is, the longer the dehydration process takes, increasing the fire-protective duration. For a fire resistance of 120 minutes, a gypsum board of 25 mm can be applied to the combustible surfaces [19].

4.5 Simulation Methods

The simulation software OZone 3.0.4, developed by ArcelorMittal in cooperation with the University of Liege and Global Research and Development Esch [2]. OZone is utilised for fire simulations following the natural fire concept. Traditionally, for structural design considerations surrounding fire, the standard fire curve, also the ISO 834 temperature-time curve, was used. This method, however, often showcases both under- and overestimations of the behaviour of the structural design regarding fire. This uncertainty often leads either to insufficient fire safety or unnecessary costs and material use. The natural fire concept provides a more realistic parametric propagation of fire derived from the rate of heat release, which allows for more accurate structural fire designs. [53] The difference between the standard fire curve ISO 834 and the natural fire concept is visualised in Figure 2.

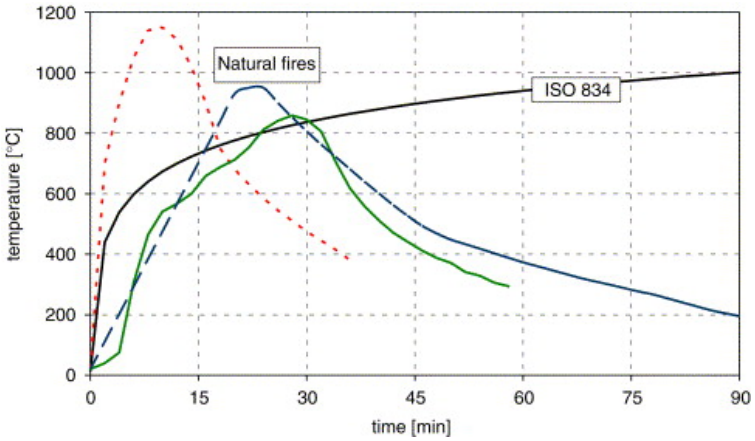

Figure 2: Standard fire curve vs. Natural fire concept [53]

Different combustion models can be applied for the fire simulations peformed in OZone. There are three types of combustion models which can be simulated: No combustion, Extended fire duration and External flaming [5]. In the No combustion model, the fire is fuel-controlled and not ventilation-controlled, implying that the model simulates negative oxygen levels when there is not sufficient oxygen from the openings in the compartment. This is not a realistic fire model, since without oxygen, a fire will eventually cease to exist. This model complies with the following equations at all times:

$$\dot{m}_f(t) = \dot{m}_{f,data}(t)$$

$$RHR(t) = RHR_{data}(t)$$

In the Extended fire duration model, it is assumed that all energy remains in the compartment, and none of the energy can escape through the openings in the compartment. This model does, however, consider the limit of oxygen availability in the compartment, thus resulting in a ventilation-controlled fire. This model is typically used in scenarios with only small openings. Since all the energy remains in the compartment, this type of model represents the worst-case scenario. When the oxygen mass is above 0 kg, and the fire is thus fuel controlled, the model complies with the following equations:

$$\dot{m}_f(t) = \dot{m}_{f,data}(t)$$

$$RHR(t) = RHR_{data}(t) = \dot{m}_f(t) \cdot H_{f,eff}$$

When the oxygen mass in the compartment is 0 kg, and the fire is ventilation controlled, the model complies with the following equations:

$$\dot{m}_f(t) = \frac{1.27}{\dot{m}_{ox.,in}(t)}$$

$$RHR(t) = \dot{m}_f(t) \cdot H_{f,eff} = \frac{1.27}{\dot{m}_{ox.,in}(t)} \cdot H_{f,eff}$$

In an External flaming model, it is assumed that, after flashover, part of the energy generated in the fire can spill out of the openings, for example, when the glazing breaks [3]. Compared to the Extended Fire Duration, this means that significant energy is lost through the openings, instead of remaining in the compartment. This model is mostly used in scenarios with large openings. This type of fire is also ventilation-controlled. When the oxygen mass is above 0 kg, and the fire is thus fuel controlled, the model complies with the following equations:

$$\dot{m}_f(t) = \dot{m}_{f,data}(t)$$

$$RHR(t) = RHR_{data}(t) = \dot{m}_f(t) \cdot H_{f,eff}$$

When all the oxygen in the compartment has been consumed, and the fire is thus ventilation controlled, the model complies with the following equations:

$$\dot{m}_f(t) = \dot{m}_{f,data}(t)$$

$$RHR(t) = \dot{m}_{ox,in}(t) \cdot H_{f,eff}$$

Usually, the reality lies between the Extended Fire Duration model and the External Flaming model.

In the model, there are several parameters which need to be defined to get return information on the fire propagation. Outside of the geometry and the materialisation of the model, which are dependent on the specific situation, there are standard values which can be implemented with regard to the behaviour of the fire. Table 1 provides the different standard values which are required for the OZone simulation models and prior calculations, based on a residential function with a timber structure and cellulosic fire behaviour.

Parameter	**Value**	**Unit**	**Source**
Variable Fire Load Density 80% fractile	870	MJ/m^2	[37]
Variable Rate of Heat Release	250	kW/m^2	[37]
Residential Fire Growth Rate	300	s	[37]
Caloric Value of Fire Wood	19	MJ/kg	[9]
Density of Wood / CLT	450	kg/m^3	[45]
Combustion factor	0.8		[11]
Stoichiometric coefficient	1.27	kg/kg	[22]

Table 1: Standard modelling and calculation values

With the model input, the simulation software provides a variety of data, such as the gas temperature, the development of the rate of heat release and the oxygen mass. This information can then again be implemented in other calculation models to derive additional data, such as the burned fire load and the equivalent fire duration. The equivalent fire duration indicates the point where the energy burned in the design/modelled fire with the natural fire concept is equivalent to the energy burned in a standard fire with the same specifications [54].

4.6 Other studies

Prior to this current study, numerous other studies have analysed the behaviour of CLT in compartment fires and its influence on the fire dynamics. In an extensive review performed by Liu et al. [23], the methods and findings of several full-scale experimental studies on the fire performance of CLT were discussed. Liu established that approximately 70% of the experiments which were reviewed focused on small compartments with an area between 0-25 m^2 and only limited ventilation. Larger open-plan compartments with high levels of ventilation, on the other hand, had only a limited number of tests attributed to them, thus requiring the extrapolation of the results from the smaller compartments to determine verified results. A lack of research was also determined in the effects of structural loading on the behaviour of the CLT structure in case of a fire, for example, how the structural load influences the capacity of the CLT during a fire, how the load influences the behaviour of connections, and how the deflection of the CLT alters. The review also indicated that self-extinction is a factor which cannot be guaranteed with set parameters, making it out to be a coincidental, fortunate situation rather than a predefined condition in a certain system.

The discovery that self-extinction is not a given based on set parameters was also determined in the experiments performed by Wiesner et al. [49], where full-scale experiments were performed on compartments with partially exposed CLT. Several scenarios were tested, and one was also tested twice in order to attempt to

verify the results. This verification test showcased that, with two experiments with the same parameters, one experiment resulted in self-extinction, while the other experiment required manual extinction as a result of continuously added fuel due to char fall-off. This comparison demonstrates that self-extinction is not a given. Furthermore, the experiments indicated that, in the case of self-extinction, after the compartment load was burned, the thermal penetration depth continued to increase, which reduced the structural integrity of the compartment and risked collapse of the compartment during the decay phase.

The experiment of Bøe et al. [8] was mainly focused on the fire spread in a large, well-ventilated, compartment with exposed CLT. The study established that a fire in a large compartment with an exposed CLT ceiling can self-extinguish. It is, however, worth noting that this specific experiment was only performed once, indicating that the self-extinguishment cannot be guaranteed. The study also noted extreme external flaming in multiple waves, on one side of the building, which was completely open aside from three concrete columns.

Similar to Wiesner et al. and Bøe et al., Medina Hevia [30] also conducted several full-scale experiments on compartments with partially exposed CLT. The experiments showed that for one exposed wall, the fire self-extinguished. However, in the scenarios of two exposed walls, both opposite and adjacent, the fire did not self-extinguish, and manual extinction was required. For the two scenarios of the two exposed walls, it was determined that the heat release in the scenario of the opposite walls was significantly higher compared to the heat release in the scenario of the adjacent walls. In view of fire safety with regard to compartments with (partially) exposed CLT, the study recommends the use of sprinklers in order to gain control over the fire without the need for external resources for manual extinction.

The recommendation on the implementation of sprinklers in a CLT compartment is also supported in the study performed by McGregor [28], where full-scale experiments were performed on both protected and exposed CLT compartments. The experiment in the protected CLT compartment with "regular" variable load exhibited self-extinction after burning the variable load, with unaffected CLT panels. However, when a propane fire was used in the protected compartment, which does not self-extinguish, the gypsum protection failed, and the CLT contributed to the fire, significantly increasing the energy release. The compartments where the CLT was exposed showcased an increase in fire growth rates, and the delamination of the CLT panels, which can cause a second flashover, resulted in an extension of the duration of the compartment fire.

As was previously stated, both char-fall off and heat-induced delamination are risks of CLT in a fire, causing additional fuel to be provided to the fire. Čoliç [12] studied the occurrence of char fall-off in CLT through experiments, and concluded that the char fall-off occurs randomly on or outside of the bond-line of two panels, but that it was not observed in panels using formaldehyde-based adhesives. With regard to delamination, it was concluded that a higher structural load results in increased delamination failures. Furthermore, Čoliç determined that the moisture content affects the behaviour of the fire. Here, it was determined that a higher moisture content results in a higher time to ignition and decreased brittle delamination of the CLT. This is supported in the study performed by Cuevas et al. [14], where it was determined that the additional moisture absorbs more energy, reducing the rate of thermal decomposition. Thus, it was concluded that moisture levels in CLT can be influential in ensuring the occurrence of flame extinction after burnout, however, flame extinction is not ensured, as was also previously discussed in other studies.

4.7 Conclusion

This literature review has elaborated on existing knowledge to demonstrate the benefits and challenges of cross-laminated timber (CLT) in fire scenarios, considering material behaviour, fire dynamics and standard practice in regulations and fire modelling.

The concepts of fire safety, which is primarily concerned with the safety of the people and other properties, and fire resilience, which also includes damage limitation, indicate different levels for evaluating the fire design of timber-based buildings. Currently, building codes are mainly focused on ensuring fire safety, but they have not yet adapted to the increasing number of buildings with flammable structures.

The overview of timber as a building material, including its composition, history and material behaviour, highlighted both its long-lived role in the built environment, as well as the challenges associated with its flammability. Historic fires involving timber buildings highlighted the importance of understanding the behaviour of the material and designing with the material accordingly. Furthermore, the review explored

the properties and behaviour of cross-laminated timber (CLT), showcasing a more complex behaviour of engineered timber products due to the combination of multiple materials. Common phenomena in the fire behaviour of CLT include char fall-off and heat delamination, which can have a significant influence on the fire dynamics. Research shows that with the use of fire protection such as gypsum boards, burning of the structure can be prevented, delayed or minimised, aiding in the fire safety and fire resilience of the building design.

Following the material-focused review, the theoretical part around fire simulations, specifically relating to the OZone software, was reviewed. Different modelling concepts and combustion models were elaborated, and standardised input parameters were defined based on existing codes and guidelines. However, due to the assumptions and simplifications associated with fire simulations, full-scale experimental research is required for validation of the simulation results. The review of existing full-scale compartment fire experiments indicated a general consensus that compartments with only one exposed CLT surface may exhibit self-extinction, however, this factor cannot be guaranteed, even under set parameters. Furthermore, the review of existing experiments provided valuable insights into the several factors of CLT influencing the fire dynamics.

Overall, existing research on the fire performance of CLT prioritises fire safety, with limited consideration of fire resilience. While numerous full-scale compartment fire experiments provide valuable insight into CLT behaviour in case of a fire, due to their high level of resource use and emissions, they allow for only limited scenarios to be investigated. On the other hand, fire simulations, which are currently underutilised, allow for a systematic and iterative exploration of fire dynamics and performance in infinite scenarios. This reveals a gap in simulation-based assessment of CLT fire resilience, providing the motivation for this research.

5 Methodology

This study focuses on the simulation of the effects of different scenarios regarding exposed and protected surfaces in a CLT compartment. This section elaborates on the methods used for both the calculations prior to the simulations, as well as the simulation process itself. Calculations prior to the simulations include the determination of the permanent fire load and the rate of heat release for each compartment scenario separately. The simulation methodology includes both the settings of the models and the iterative process. Subsequently, the determination of the equivalent fire duration is discussed.

The scenarios which are covered in this study include a traditional non-flammable compartment, a CLT compartment where all surfaces are exposed, a CLT compartment where only the ceiling is exposed, a CLT compartment where only one wall is exposed, a CLT compartment where two opposite walls are exposed, a CLT compartment where both the ceiling and one wall are exposed, and a CLT compartment where both the ceiling and two opposite walls wall are exposed. The different compartment variants are visualised in Figure 3.

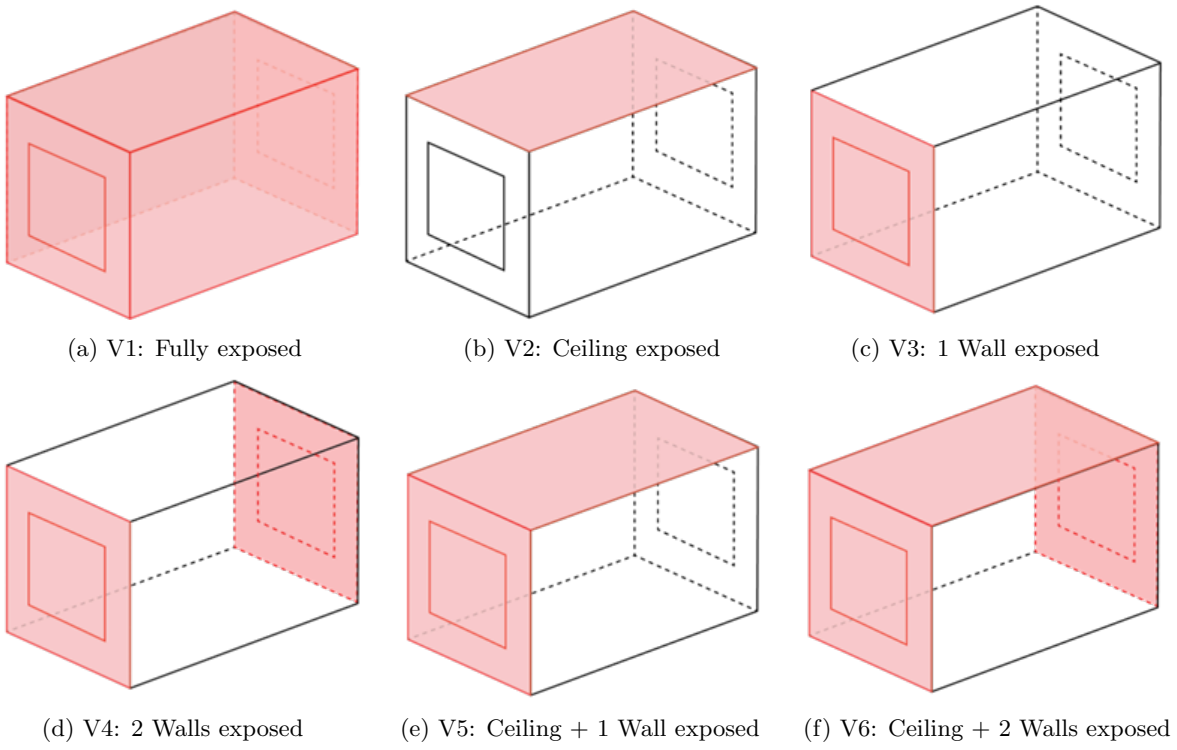

(a) V1: Fully exposed (b) V2: Ceiling exposed (c) V3: 1 Wall exposed

(d) V4: 2 Walls exposed (e) V5: Ceiling + 1 Wall exposed (f) V6: Ceiling + 2 Walls exposed

Figure 3: Simulation Variants

5.1 Compartment Fire Load

As was previously discussed in the literature review, aside from the average variable fire load, exposed CLT surfaces add a permanent fire load to the total fire load of the building. Research shows that it is important that the fuel load of the exposed CLT at any time during the fire is implemented in parametric, natural, fire simulations [29]. The average variable fire load is determined in NEN 6055 for residential purposes at 80% fractile [37]. The permanent fire load as a result of the exposed CLT structure is determined with the use of Equation 1.

$$p_{perm} = \frac{H \cdot \rho \cdot \sum(A_i \cdot d_i)}{A_f} \quad MJ/m^2 \tag{1}$$

In this equation, H is the caloric value used for firewood in massive timber buildings of 19 MJ/kg, as determined in NEN-6081 [9]. Using ρ, the average density of CLT of 450 kg/m^3, and A_i and d_i, the area in m^2 and thickness in m of the exposed CLT surface, the total mass of the exposed CLT is determined, where i indicates the different surfaces. A_f is the floor area of the compartment in m^2, which is used to determine the load per m^2 of floor area of the compartment. Furthermore, with a combustion efficiency of 0.8, as determined in EN-1991-1-2: Eurocode 1, the total burnable permanent fire load can be determined [11]. The implementation of the permanent fire load in the OZone simulations does not automatically consider the combustion efficiency. The burnable permanent fire load is therefore determined prior to the simulations. The calculated values of the total permanent fire load and the burnable permanent fire load are elaborated in Table 2.

Compartment	**Total permanent fire load** $[MJ]$	**Burnable permanent fire load** $[MJ]$
V1	179699.6	143759.7
V2	95760.0	76608.0
V3	13754.8	11003.9
V4	27509.6	22007.7
V5	109514.8	87611.9
V6	123269.6	98615.7

Table 2: Results Permanent Fire Load Calculation

5.2 Rate of Heat Release

In order to determine the rate of heat release (RHR) input in the OZone simulations, data stemming from a previous study conducted by S. van Poppel is analysed and transformed for use in this specific study. Van Poppel performed experiments on the mass loss of CLT samples for different values of received radiation flux [39]. The results from the experiments are elaborated in Table 3. Here $m_{l,m,avg}$ is the average mass loss of 1 m^2 of sample per minute, which was determined through averaging the mass loss for the separate samples for each radiation flux. $m_{l,A,avg}$ is the average mass loss of 1 m^2 of sample for the entire duration of the exposure, which was determined by multiplying $m_{l,m,avg}$ by the duration of the radiation exposure. The results only contain three points of received radiation flux out of the five measured points, since the two remaining data points where not verified due to their large variations.

Parameter	**Unit**			
Maximum received radiation flux ($q_{r,max}$)	kW/m^2	30	4	3
Distance between the panels (d)	m	0.25	0.89	1.07
Duration of the exposure (t)	min	30	120	120
Average mass loss of the sample ($m_{l,m,avg}$)	$kg/min \cdot m^2$	0.2287	0.0215	0.00975
Average mass loss of the sample ($m_{l,A,avg}$)	kg/m^2	6.861	2.580	1.170

Table 3: Experiment Results S. van Poppel [39]

The received radiation flux on the sample is determined with the use of a view-factor calculation method in combination with the known produced radiation and the distance between the panels. The view-factor indicates the fraction of radiation which leaves the area producing the radiation and is intercepted by the receiving area [42]. In the study by Van Poppel, the calculation point adopted was the middle-point of the

CLT sample and radiation panel, when they were centred opposite each other. This choice of calculation point results in the maximum received radiation flux. However, for this study, the aim is to determine and utilise the average received radiation flux. The average received radiation flux is determined using the same view-factor calculation method, however, with the calculation point set where the centre of a quarter of the CLT sample would coincide with the radiation panel. The determination of the geometric data for both the maximum, applying the centre calculation point, and the average, applying the previously discussed calculation point, received radiation flux is shown in Table 4. Here h_s and b_s respectively indicate the total height and width of the CLT sample, whereas h_p and b_p respectively indicate the total height and width of the radiation panel. The geometric data of the CLT sample and the radiation panel are provided in Figure 4.

View-factor type	h_1	h_2	b_1	b_2
Maximum [39]	$\frac{1}{2} \cdot h_s$	$\frac{1}{2} \cdot h_s$	$\frac{1}{2} \cdot b_s$	$\frac{1}{2} \cdot b_s$
Average	$\frac{1}{2} \cdot h_p - \frac{1}{4} \cdot h_s$	$h_p - h_1$	$\frac{1}{2} \cdot b_p - \frac{1}{4} \cdot b_s$	$b_p - b_1$

Table 4: Geometric data for maximum and average received radiation flux

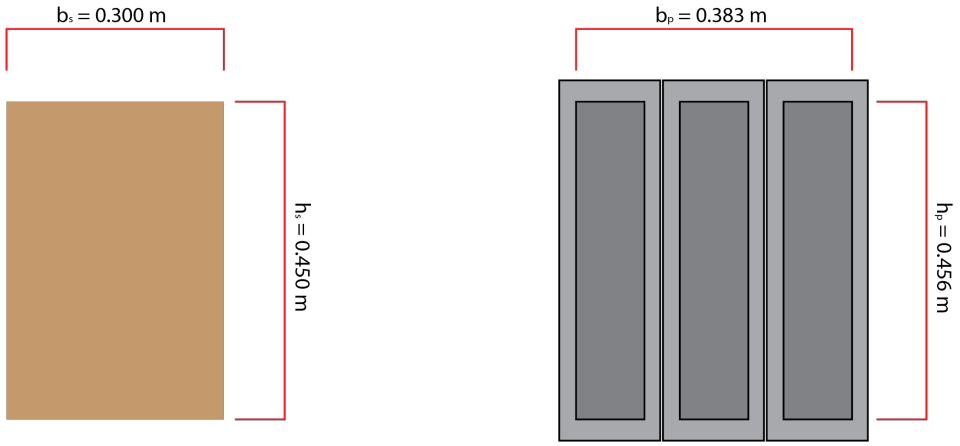

(a) CLT sample (b) Radiation panel

Figure 4: Geometry

Together with the distance between the planes (d), h_1, h_2, b_1 and b_2 are used to determine the view-factors of each quadrant, namely f_A, f_B, f_C and f_D. The overall view-factor is determined by the summation of the view-factors of all the quadrants, f_{tot}. The view factor is calculated with the use of a calculation model, of which the calculation methods are elaborated in Appendix A. Using the calculated view-factor (f_{tot}), the radiation flux of the source (q_{source}) and the transmission coefficient (τ), the received radiation flux is determined using Equation 2.

$$q_r = q_{source} \cdot \tau \cdot f_{tot} \quad kW/m^2 \tag{2}$$

The average received radiation flux fitting the experiments of Van Poppel is then determined using the previously stated equations and the data determined in Table 3 and Table 4. First, the radiation flux of the source is determined through backwards computation, where the maximum received radiation flux from Van Poppel is matched to the corresponding source radiation flux, utilising the maximum geometric data and the distance between the planes. With the source radiation flux known, together with the average geometric data and the plane distance, the average received radiation flux can be determined. The corrected results by Van Poppel for the average received radiation flux are provided in Table 5.

Parameter	Unit			
Average received radiation flux ($q_{r,avg}$)	kW/m^2	25.6	3.83	2.92
Distance between the panels (d)	m	0.25	0.89	1.07
Duration of the exposure (t)	min	30	120	120
Average mass loss of the sample ($m_{l,m,avg}$)	$kg/min \cdot m^2$	0.2287	0.0215	0.00975
Average mass loss of the sample ($m_{l,A,avg}$)	kg/m^2	6.861	2.580	1.170

Table 5: Corrected Experiment Results S. van Poppel [39]

The calculated average received radiation flux is utilised in order to determine the radiative gas temperature, through Equation 3. Here, q_r is the average received radiation flux in W/m^2, e is the emission-absorption coefficient of 1, σ is the Stefan-Boltzmann constant of $5.67 \cdot 10^8$ W/m^2K^4, T_a is the ambient temperature of 293 K, and T_r is the radiative gas temperature in K.

$$q_r = e \cdot \sigma \cdot (T_r^4 - T_a^4) \quad kW/m^2 \tag{3}$$

Aside from the average received radiation flux and the radiative gas temperature, the RHR of the CLT in the compartment is to be determined for each received radiation flux. With the RHR known for each received radiation flux, depending on the radiative gas temperature in the simulation, the RHR for the compartment can be adjusted accordingly through an iterative process. In order to determine the RHR for the CLT in a specific compartment, first, the produced RHR of the experiments from van Poppel is determined, employing Equation 4. Here H is the caloric value used for cellulose-based building materials in MJ/kg, as determined in NEN-6055 [37], $m_{l,A,avg}$ is the average mass loss per m^2 of sample in kg/m^2 for the complete time duration, and t is the time duration of the radiation exposure in *sec*. With the use of this data, the produced RHR is transformed to be accurate for the compartment, utilising Equation 5. Here $\sum A_i$ is the total exposed CLT surface area in the compartment in m^2, and A_f is the floor area of the compartment in m^2.

$$RHR_s = \frac{(H \cdot 1000) \cdot m_{l,A,avg}}{t} \quad kW/m^2 \tag{4}$$

$$RHR_c = \frac{RHR_s \cdot \sum(A_i)}{A_f} \quad kW/m^2 \tag{5}$$

With the known data points of the average received radiation flux and the RHR for the CLT in the specified compartment, graphs are drafted, with the received radiation flux on the x-axis and the RHR for the CLT in the specified compartment on the y-axis. With a logarithmic scale with base 2 on the x-axis and a logarithmic trend-line, the resulting linear graph and the equation of the trend-line are used to determine the RHR for the CLT in the specified compartment where the average received radiation flux is outside the known data points. The graphs elaborating on the connection between the received radiation flux and the RHR for the CLT are provided in Appendix B. The resulting trend-line equations, as shown below, are used for determining the time intervals for each scenario, further elaborated in Paragraph 5.3.

Compartment	Trend-line equation
V1	$RHR_c = 74.836 \cdot ln(q_r) - 78.693 \quad kW/m^2$
V2	$RHR_c = 32.895 \cdot ln(q_r) - 34.59 \quad kW/m^2$
V3	$RHR_c = 6.8727 \cdot ln(q_r) - 7.2269 \quad kW/m^2$
V4	$RHR_c = 13.745 \cdot ln(q_r) - 14.454 \quad kW/m^2$
V5	$RHR_c = 39.768 \cdot ln(q_r) - 41.817 \quad kW/m^2$
V6	$RHR_c = 46.641 \cdot ln(q_r) - 49.044 \quad kW/m^2$

Table 6: Rate of Heat Release vs Received Radiation Flux equations

5.3 Simulation Model

The simulations are conducted in OZone using Annex E based on EN 1991-1-2, or with a User Defined Fire, together with the external flaming combustion model. With Annex E, the Fire Growth Rate, RHR, Fire Load, as well as information on the safety factors, the fire, design fire load and the combustion are required for modelling. With Annex E, the behaviour of the fire in the compartment for the variable fire load is simulated. In the User Defined Fire, the time intervals and corresponding RHR, as well as information on the fire and combustion, are required. The User Defined Fire allows for the manual addition of the permanent fire load of the CLT to the variable fire behaviour, as will be further elaborated on in this paragraph.

A standard compartment geometry was applied, with a height, depth and length of 3, 7 and 10 m, respectively. The compartments are modelled with a flat roof and two equally sized openings in the shorter walls. The openings in the facades are adjusted to the worst-case scenario for a fire with variable load only, so the fire is fuel-controlled post-flashover. For all scenarios, both openings are sized at 1.5 m high and 4.25 m wide, situated at a height of 0.5 m. The materials, standardised and provided through OZone, are elaborated in Table 7 for each different type of scenario. For constructions with multiple materials, the materials are provided ordered from interior to exterior. The thickness of the layers of CLT is based on average thicknesses utilised in CLT structures, with 0.11 m for walls and 0.16 m for floors and ceilings [48].

Construction type	Materialisation
Exposed CLT wall	0.11 m Normal Wood
Protected CLT wall	0.025 m Gypsum board [EN12524] and 0.11 m Normal Wood
Exposed CLT ceiling	0.16 m Normal Wood and 0.10 m Normal weight Concrete [EN1994-1-2]
Protected CLT ceiling	0.025 m Gypsum board [EN12524] and 0.16 m Normal Wood and 0.10 m Normal weight Concrete [EN1994-1-2]
CLT floor	0.10 m Normal weight Concrete [EN1994-1-2] and 0.16 m Normal Wood

Table 7: Material selection OZone simulations

Using the information received from the trend-line in Appendix B, in combination with the radiative gas temperature calculation following from Equation 3, the temperature limits and permanent RHR for the CLT in the specified compartment can be determined. For each compartment with exposed CLT surfaces, eight different temperature intervals (T_r) are determined, considering an approximate continuous difference of the permanent RHR for the CLT in the specified compartment (RHR_c). The interval data, with iteration step i, used for the simulations for all six models, is provided in Table 8 through Table 13.

Parameter	Unit	i=0	i=1	i=2	i=3	i=4	i=5	i=6	i=7
$q_{received}$	kW/m^2	160	82	42	21.5	11	5.6	4.6	3.8
T_r	$^{\circ}C$	$\geq$1023.9	$\geq$825.0	$\geq$657.0	$\geq$515.5	$\geq$396.9	$\geq$297.8	$\geq$272.4	$\geq$249.2
RHR_c	kW/m^2	300.39	250.46	200.48	150.47	100.41	49.99	35.29	21.02
RHR_c	MW	21.0271	17.5321	14.0339	10.5328	7.0289	3.4989	2.4705	1.47156

Table 8: Interval simulation data CLT fully exposed

Parameter	Unit	i=0	i=1	i=2	i=3	i=4	i=5	i=6	i=7
$q_{received}$	kW/m^2	151	82	44	24	13	7	5.3	3.8
T_r	$^{\circ}C$	$\geq$1005.3	$\geq$825.0	$\geq$667.8	$\geq$537.1	$\geq$424.5	$\geq$328.4	$\geq$290.5	$\geq$249.2
RHR_c	kW/m^2	130.45	110.37	89.89	69.95	49.78	29.42	20.27	9.32
RHR_c	MW	9.1317	7.7258	6.2924	4.8966	3.4849	2.0595	1.4189	0.6527

Table 9: Interval simulation data CLT ceiling exposed only

Parameter	Unit	i=0	i=1	i=2	i=3	i=4	i=5	i=6	i=7
$q_{received}$	kW/m^2	157	82	42	22	11.5	6	4.8	3.8
T_r	$^{\circ}C$	$\geq$1017.8	$\geq$825.0	$\geq$657.0	$\geq$519.9	$\geq$404.1	$\geq$307.0	$\geq$277.8	$\geq$249.2
RHR_c	kW/m^2	27.52	23.06	18.46	14.02	9.56	5.09	3.55	1.95
RHR_c	MW	1.9266	1.6141	1.2923	0.9812	0.6691	0.3561	0.2488	0.1364

Table 10: Interval simulation data CLT one wall exposed

Parameter	Unit	i=0	i=1	i=2	i=3	i=4	i=5	i=6	i=7
$q_{received}$	kW/m^2	157	88	49	28	15	8.5	5.7	3.8
T_r	$^{\circ}C$	$\geq$1017.8	$\geq$844.5	$\geq$693.2	$\geq$568.4	$\geq$449.1	$\geq$356.8	$\geq$300.1	$\geq$249.2
RHR_c	kW/m^2	55.04	47.09	39.04	31.35	22.77	14.96	9.47	3.90
RHR_c	MW	3.8531	2.7327	2.1943	1.5938	1.0473	0.6628	0.2727	

Table 11: Interval simulation data CLT two walls exposed

Parameter	Unit	i=0	i=1	i=2	i=3	i=4	i=5	i=6	i=7
$q_{received}$	kW/m^2	160	85	45	24	13	6.9	5.1	3.8
T_r	$^{\circ}C$	$\geq$1023.9	$\geq$834.9	$\geq$673.0	$\geq$537.1	$\geq$424.5	$\geq$326.4	$\geq$285.5	$\geq$249.2
RHR_c	kW/m^2	160.01	134.86	109.57	84.57	60.19	34.99	22.97	11.27
RHR_c	MW	11.2009	9.4401	7.6696	5.9197	4.2130	2.4497	1.6082	0.7891

Table 12: Interval simulation data CLT ceiling and one wall exposed

Parameter	Unit	i=0	i=1	i=2	i=3	i=4	i=5	i=6	i=7
$q_{received}$	kW/m^2	168	88	46	24	13	6.7	5	3.8
T_r	$^{\circ}C$	$\geq$1039.8	$\geq$844.5	$\geq$678.2	$\geq$537.1	$\geq$424.5	$\geq$322.2	$\geq$283.0	$\geq$249.2
RHR_c	kW/m^2	189.94	159.78	129.53	99.18	70.59	39.67	26.02	13.22
RHR_c	MW	13.2960	11.1848	9.0669	6.9429	4.9412	2.7771	1.8215	0.9255

Table 13: Interval simulation data CLT ceiling and two walls exposed

Prior to the simulations, including the permanent fire load of the CLT, simulations are performed with only the variable fire load using the Annex E method as previously described. This determines the fire behaviour based on the t^2 design curve, which estimates the development of the fire pre-flashover [10]. Here, the Fire Growth Rate was set to 300 s, the RHR was set to 250 kW/m^2, and the Variable Fire Load was set to 870 MJ/m^2. These values are based on the average natural fire parameters as determined in the Dutch standard NEN-1991-1-2 as of 2018 [21]. The variable fire load simulations are performed with the materials as determined in Table 7.

With the simulation results of the variable fire load as a base, an iterative process of the addition of the RHR_c is used to determine the complete natural fire behaviour in the compartment. The iterative process starts with the RHR of the variable load simulation. Starting at the moment of flashover, the maximum $RHR_{c,i}$, as determined in Table 8 through Table 11, is added to the RHR of the variable load simulation, up until the point in time where the burnable permanent fire load would be burned up, assuming that the $RHR_{c,i}$ would remain the same throughout the entire fire. This point in time is calculated using Equation 6.

$$t_{burned,i} = \frac{p_{perm,i}}{RHR_{c,i}} \quad [s] \tag{6}$$

After this point in time, the $RHR_{c,i}$ added to the RHR from the variable fire load simulation is set to 0 MW. This data is then implemented in the User Defined method within the OZone fire simulation for the specified compartment, and the fire is set to the external flame concept. This simulation results in, among other data, a Hot Zone Temperature graph, which aids in determining the point in time at which the gas temperature is below the minimum temperature of the temperature interval set for the maximum $RHR_{c,i}$. In the following phase, the $RHR_{c,i}$ is maintained until the previously defined point in time where the gas temperature is below the minimum value of the temperature interval. From this point in time, the $RHR_{c,i}$ is reduced to the value belonging to the temperature interval below the maximum, $RHR_{c,i+1}$. Here, it is calculated how much of the burnable permanent fire load has already been burned up under the influence of the maximum $RHR_{c,i}$, and the fire load which remains, as elaborated in Equation 7.

$$p_{perm,i+1} = p_{perm,i} - (t_{<T_{min},i} - t_{start,i}) \cdot RHR_{c,i} \quad [MJ] \tag{7}$$

With this known fire load, it is determined at what point in time the remaining burnable permanent fire load would be burned up with the $RHR_{c,i+1}$ of the next temperature interval, and thus when the $RHR_{c,i+1}$ is to be set to 0 MW. Again, this data is then implemented in the User Defined fire method in OZone, and the point in time where the gas temperature is below the minimum of the temperature interval is determined. This process is repeated, either until the total burnable permanent fire load is burned up, or until the temperature after the last $RHR_{c,i}$ is below 249.2 °C, meaning that the $RHR_{c,i}$ is set to 0 MW. At the end of the process, the % of the exposed CLT structure remaining after the fire is determined using Equation 8 and the burned fire load is determined using Equation 9.

$$p_{remaining} = \frac{p_{perm,end}}{p_{perm,tot}} \cdot 100\% \quad [\%] \tag{8}$$

$$p_{burned} = p_{perm,tot} - p_{perm,end} \quad [MJ] \tag{9}$$

This value is verified through integration under the RHR graph following from the final OZone simulation of the iterative process, following the calculation in Equation 10. This calculation provides the total burned fire load, including both the variable and permanent fire load. By performing this calculation for the variable simulations separately and deducting that value from the total burned fire load, the burned permanent fire load can be determined.

$$p_{burned,v} = \frac{\int_{t=0}^{\infty} RHR(t)dt}{10^6} \quad [MJ] \tag{10}$$

5.4 Equivalent Fire Duration

The equivalent fire duration for each scenario can be determined using the data resulting from the simulations. This can be implemented in the calculation model for the equivalent fire duration provided by Brandveilig Met Staal [47]. This calculation model determines the equivalent fire duration following Equation 11, which determines the total energy in the compartment through integration. Here m_{ox} is the oxygen mass in kg, c_v is the specific heat capacity of air at constant volume at 719.7 J/kgK, T_r is the gas temperature in K and T_a is the ambient temperature at 293 K.

$$E = \int_{t=0}^{t_{end}} m_{ox} \cdot c_v \cdot (T_r - T_a)dt \quad [J] \tag{11}$$

The total energy for the compartment in the natural fire concept and following the standard fire curve is compared, and the equivalent fire duration is then the time at which the energy in the compartment is the same for both the natural fire concept and the standard fire curve.

6 Results

In OZone, multiple scenarios of iterative simulations as well as the baseline simulation were conducted following the methodology determined in section 5. Initially, the baseline situation was simulated, with only variable load contribution to the fire since all surfaces were protected. The report of the simulation of the baseline model is provided in Appendix C. After all the variable load was burned, the fire self-extinguished. The CLT behind the protection remained unaffected, since the equivalent fire duration at 70 minutes is below the 120-minute fire resistance of the protection. The iterative simulations of the scenarios with exposed CLT surfaces demonstrated a clear connection between the exposed surfaces and the amount of burned permanent fire load, as elaborated in Table 14.

Here, Total Perm. FL is the total available permanent fire load as a result of the exposed CLT surfaces. Since the combustion efficiency is assumed at 80%, as elaborated in Chapter 4, the total burnable permanent fire load (Burnable Perm. FL) is determined as 80% of the total permanent fire load. The Burned Perm. FL indicates the amount of *MJ* which was burned during the fire, and how much this is compared to the available burnable permanent fire load. The Eq. FD indicates the equivalent fire duration for each scenario.

	Total Perm. FL	**Burnable Perm. FL**	**Burned Perm. FL**		**Eq. FD**
Compartment	[MJ]	[MJ]	[MJ]	[%]	[min]
V1	179699.6	143759.7	143825.3	100%	144
V2	95760.0	76608.0	45276.3	59%	104
V3	13754.8	11003.9	6308.4	57%	74
V4	27509.6	22007.7	13243.8	60%	77
V5	109514.8	87611.9	88040.5	100%	150
V6	123269.6	98615.7	98922.2	100%	146

Table 14: Simulation Results Summary

The results imply that *V2 – V4* are the three scenarios which do not experience a burn-down scenario, since not all of the permanent fire load is burned. *V2* and *V3* both only have one exposed surface, and *V4* has two exposed surfaces, which are opposite each other. The resulting equivalent fire duration of each of these scenarios indicates a value below 120 minutes. The other three scenarios with two or more exposed surfaces (*V1, V5 & V6*) all experience a complete burn-down scenario with an equivalent fire duration of above 120 minutes. Through the verification method, it was confirmed that the calculated and integrated values for all scenarios differ less than 0.1% compared to the total permanent fire load.

Figure 5 showcases the simulated temperature evolution of all the scenarios. This graph also clearly shows that *V1, V5 & V6* all experience a burn-down scenario, since the temperature suddenly drops drastically, indicating that all the available fire load has been burned. *V2 – V4*, on the other hand, show a gradual temperature decrease post-flashover, indicating the gradual decay of the fire.

Figure 6 expresses the thermal load in minutes standard fire for all six scenarios. The results indicate an increasing fire duration in standard fire minutes with an increasing exposed CLT surface. *V3 & V4*, closely followed by *V2*, indicate a significantly shorter fire duration, compared to *V1, V5 & V6*. Indicating a similar trend as illustrated in Figure 5.

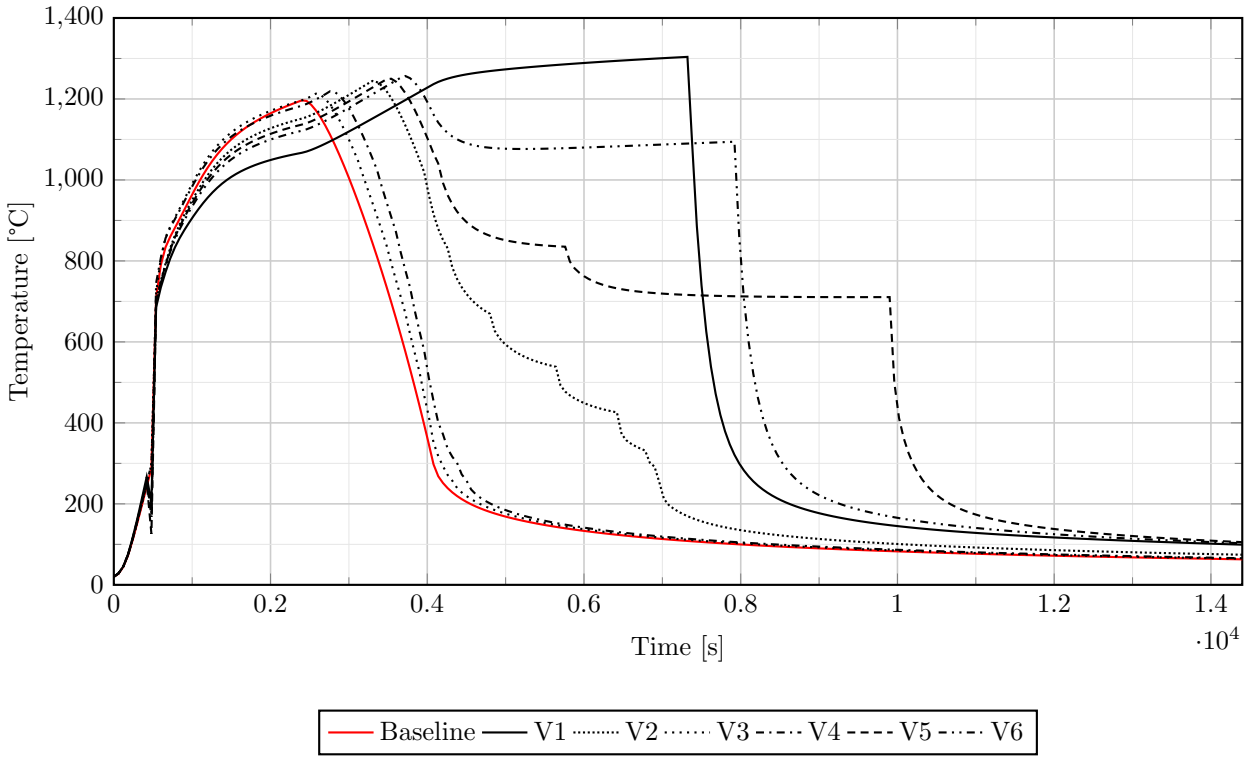

Figure 5: Temperature Evolution over Time for Compartments V1–V6

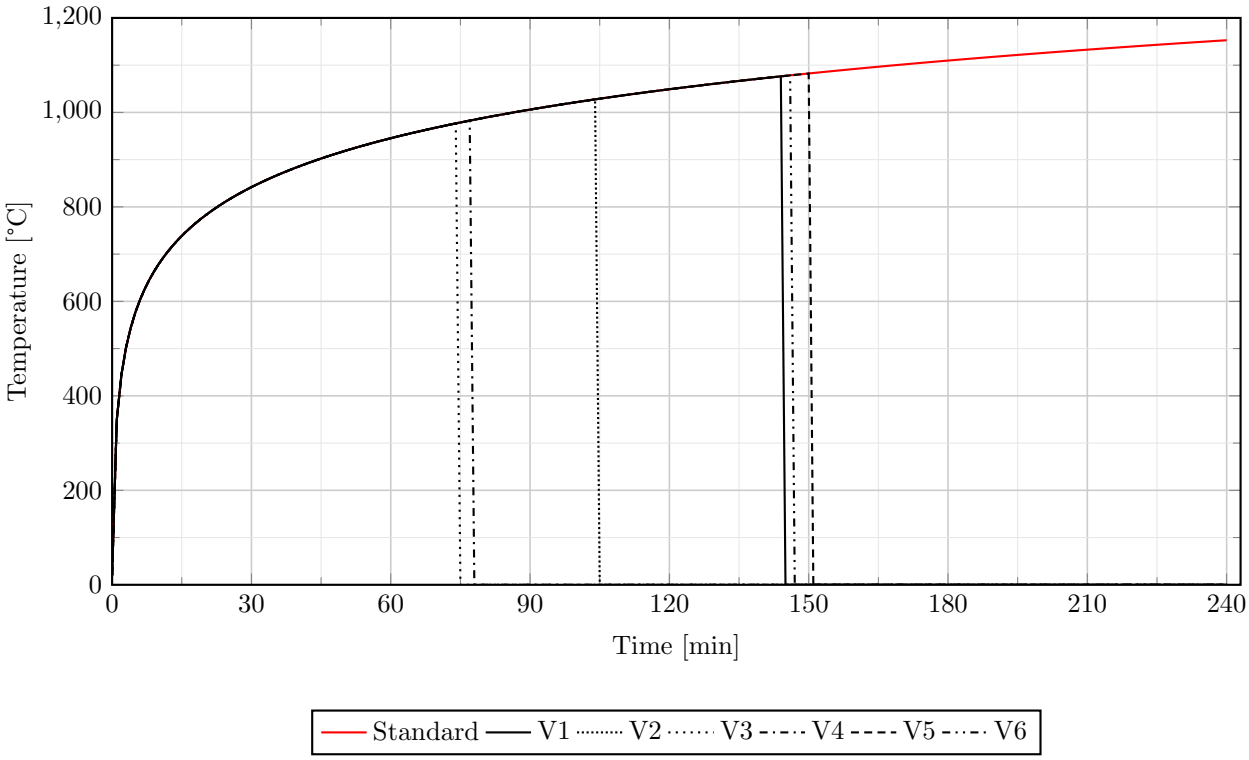

Figure 6: Thermal Load in Minutes Standard Fire for Compartments V1–V6

7 Discussion

The results from the simulations demonstrated that, for only one exposed CLT surface, there is no burn-down scenario, indicating it to be a fire-resilient compartment. Aside from the burned permanent fire load, the equivalent fire duration also remains under 120 minutes, indicating that the fire-resistant gypsum board protection would not yet have failed, and would thus not have exposed additional CLT surfaces to the fire. The scenario with two exposed walls also indicates that not all permanent fire load is burned, as well as an equivalent fire duration below 120 minutes. However, due to the simplicity of the modelling software, the effects of the radiation from the two surfaces on each other are unknown, hence the results in this scenario are possibly too positive. The other three scenarios with two or more exposed CLT surfaces each display a burn-down scenario, indicating that these three scenarios are not fire-resilient. Furthermore, the equivalent fire duration is above 120 minutes, which could indicate that the fire-resistant gypsum boards would fail during the fire, adding additional fire load to the fire. The large variation in equivalent fire duration between all scenarios indicate that the same level of gypsum fire board protection is not needed for all scenarios. Instead, scenarios with a shorter fire duration could also function with gypsum fire protection with a lower duration of fire resistance, thus also requiring fewer materials. These results are valuable for small residential compartments with large daylight openings.

These results are consistent with the existing research as elaborated in the literature. The full-scale experiments conducted in compartments with (partially) exposed CLT imply possible self-extinguishment in the case of a singular exposed surface, whereas multiple surfaces required manual extinguishment. This is in line with the simulations performed in this study, which also suggest a scenario of self-extinguishment with one exposed surface, and no self-extinguishment with multiple exposed surfaces. However, the experiments also concluded that self-extinguishment of a CLT fire is not guaranteed under set parameters, so it is important to take this into account when interpreting the results of this study.

When interpreting the findings of this research, several limitations should be acknowledged. First of all, it is important to note that this study is based on general, standardised data following the existing standards and recommendations at the time of this study. Furthermore, in the determination of the rate of heat release, there was only a minimal number of data points available, which could have influenced the validity of the calculation and simulation results. Due to limitations with regard to the extent of the experiments required for this data, it was not possible to provide additional data points. Aside from this, as was previously discussed, the reality of natural fires lies between the extended fire duration and the external flaming simulation model, indicating possible deviation from a real-life fire. Additionally, due to the simplicity of the simulation software, the effects of the radiation of adjacent and opposite exposed surfaces on each other in a fire are unknown, possibly conveying overly positive results. The effects of the adhesive layer and resulting delamination or char fall-off could not be implemented in the simple software and are thus not taken into account in the results. Similarly, the failure of the fire-resistant gypsum board protection has not been taken into account in the simulations, which could have influenced the intensity and duration of the fire for fires exceeding a duration of 120 minutes. Further research is recommended on these effects of the radiation, adhesives and the failure of the gypsum, in order to determine whether or not fire-resilience is influenced.

8 Conclusion

In this study, the primary aim was to address the changes of structural fire design with the increasing use of sustainable bio-based building materials such as CLT, guided by the research question:

> *"How does the fire resilience of a CLT compartment differ from a non-flammable compartment under simulated natural fire conditions, and how can fire-resistant materials improve the fire performance of the CLT compartment?"*

Alongside the primary aim, this study also explored how CLT and the implementation of fire-resistant materials influence the fire dynamics, such as temperature evolution and rate of heat release, through literature and simulations.

In the literature review, it was determined that fire safety and fire resilience are very different concepts with regard to the view on structural fire design. Where fire safety is mainly focused on the safety of people and other properties, the concept of fire resilience has the main aim that there should only be minimal restoration to the building structure in order for it to be functional again, instead of accepting the need for demolition post-fire. A fire-resilient building would then not only save in costs, since only restoration is required instead of full demolition and rebuilding, but it would also ensure a more sustainable material use. Sustainable material use is also one of the main reasons why nowadays more and more buildings are built with sustainable and bio-based materials such as timber. History shows that flammable building structures of timber, compared to non-flammable structures of bricks, have been involved in many widespread fires, also emphasising the need for sufficient fire safety with the increasing number of sustainable buildings.

Cross-laminated timber (CLT) is a widely used engineered timber product. Due to its layered structure, this type of timber poses additional challenges in a fire due to phenomena such as heat delamination and char fall-off, which can significantly influence the fire behaviour. Previous experimental studies indicated that self-extinction is not a guaranteed factor, but that compartment fires with a singular exposed surface have shown to self-extinguish, whereas compartment fires with multiple exposed surfaces require manual extinction. The use of fire protection, such as gypsum boards, has therefore been identified as an important factor in improving both fire safety and fire resilience.

To further investigate the effects of fire protection in a CLT compartment, simulations were performed in the OZone fire simulation software, utilising the natural fire concept and the external flaming combustion model. An iterative simulation process was used in order to provide a realistic fire evolution. The results showed that scenarios with one exposed CLT surface exhibited self-extinction before the complete permanent compartment fire load was burned and before the gypsum fire protection boards on the other surfaces would fail, indicating fire-resilient behaviour. The scenarios with multiple exposed CLT surfaces, however, typically showcased a burn-down scenario before self-extinction, an equivalent fire duration longer than the fire resistance of the gypsum boards, and exposure of additional (previously protected) surfaces, which would not be considered fire-resilient. One exception was the scenario with two opposite exposed walls, which showcased a similar self-extinction trend as the scenarios with one exposed surface, however the effects of the walls on each other are unknown, and therefore the result could be too conservative. When taking into account a shorter fire duration in the case of less exposed CLT surfaces, the thickness of the gypsum fire protection could be reduced accordingly, since the present simulations include gypsum with a higher duration of fire resistance than required. Overall, this study demonstrates the potential of fire simulation approaches to assess the fire safety and fire resilience of CLT compartments under natural fire conditions, highlighting the importance of the use of fire protection for achieving fire-resilient timber-based building designs.

References

[1] Y. Alia Syahirah, U. M.K. Anwar, Lee Sh, C. B. Ong, M. Asniza, and M. T. Paridah. The properties of Cross Laminated Timber (CLT): A review. *International Journal of Adhesion and Adhesives*, 138:103924, 3 2025. ISSN 0143-7496. doi: 10.1016/J.IJADHADH.2024.103924. URL https://www.sciencedirect.com/science/article/pii/S0143749624003063.

[2] ArcelorMittal. Design Software - Ozone, 2025. URL https://sections.arcelormittal.com/design_aid/design_software/EN.

[3] Eleni Asimakopoulou, Konstantinos Chotzoglou, Dionysios Koliatis, and Maria Founti. Characteristics of Externally Venting Flames and Their Effect on the Façade: A Detailed Experimental Study. *Fire Technology*, 52:2043–2069, 3 2016. ISSN 0015-2684. doi: 10.1007/s10694-016-0575-5. URL https://link.springer.com/article/10.1007/s10694-016-0575-5.

[4] Alastair I. Bartlett, Rory M. Hadden, Juan P. Hidalgo, Simón Santamaria, Felix Wiesner, Luke A. Bisby, Susan Deeny, and Barbara Lane. Auto-extinction of engineered timber: Application to compartment fires with exposed timber surfaces. *Fire Safety Journal*, 91:407–413, 7 2017. ISSN 03797112. doi: 10.1016/j.firesaf.2017.03.050.

[5] Bauforum Stahl. OZone V3 User Manual. Technical report. URL https://bauforumstahl.de/wp-content/uploads/2025/05/LOCAFI__Deliverable_D1.4_Software_OZone_DE.pdf.

[6] BBC. Notre-Dame: Massive fire ravages Paris cathedral, 4 2019. URL https://www.bbc.com/news/world-europe-47941794.

[7] BBC. The Great Fire of London, 2025. URL https://www.bbc.co.uk/bitesize/articles/z7j6s82#znhvcxs.

[8] Andreas Sæter Bøe, Kathinka Leikanger Friquin, Daniel Brandon, Anne Steen-Hansen, and Ivar S. Ertesvåg. Fire spread in a large compartment with exposed cross-laminated timber and open ventilation conditions: #FRIC-01 – Exposed ceiling. *Fire Safety Journal*, 140, 10 2023. ISSN 03797112. doi: 10.1016/J.FIRESAF.2023.103869.

[9] Daniel Brandon, Pascal Steenbakkers, and Ijsbrand van Straalen. Brandveiligheid massieve houtbouw Achtergrondrapport bij NTA 6125 (concept). Technical report, ARUP, 2 2025. URL https://www.nen.nl/media/wysiwyg/NTA_6125_Achtergrond_rapport_-_Nederlandse_concept_vertaling.pdf.

[10] Alex C. Bwalya. An overview of design fires for building compartments. *Fire Technology*, 44(2):167–184, 6 2008. doi: 10.1007/s10694-007-0031-7. URL http://laws.justice.gc.ca/en/showtdm/cs/C-42http://lois.justice.gc.ca/fr/showtdm/cs/C-42.

[11] CEN European Committee for Standardisation. EN 1991-1-2: Eurocode 1: Actions on structures - Part 1-2: General actions - Actions on structures exposed to fire. 11 2002.

[12] Antonela Čolić. STUDY OF THE CHAR FALL-OFF PHENOMENON IN CROSS-LAMINATED TIMBER UNDER FIRE CONDITIONS. Technical report, 2020. URL https://www.researchgate.net/publication/353265274_International_Master_of_Science_in_Fire_Safety_Engineering_Thesis_Study_of_the_char_fall-off_phenomenon_in_cross-laminated_timber_under_fire_conditions.

[13] Roy Crielaard, Jan Willem van de Kuilen, Karel Terwel, Geert Ravenshorst, and Pascal Steenbakkers. Self-extinguishment of cross-laminated timber. *Fire Safety Journal*, 105:244–260, 4 2019. ISSN 03797112. doi: 10.1016/j.firesaf.2019.01.008.

[14] Juan Cuevas and Cristian Maluk. The role of moisture on the flame extinction potential of Cross-laminated Timber. *Fire Safety Journal*, 141, 12 2023. ISSN 03797112. doi: 10.1016/J.FIRESAF.2023.103937.

[15] Andrea. Deplazes. *Constructing architecture : materials, processes, structures : a handbook*. Birkhauser, Basel, fourth edition, 2018. ISBN 9783035616699.

[16] Richard Emberley, Arne Inghelbrecht, Zeyu Yu, and José L. Torero. Self-extinction of timber. *Proceedings of the Combustion Institute*, 36(2):3055–3062, 2017. ISSN 15407489. doi: 10.1016/j.proci.2016.07.077.

[17] Ali Akbar Firoozi, Ali Asghar Firoozi, D. O. Oyejobi, Siva Avudaiappan, and Erick Saavedra Flores. Emerging trends in sustainable building materials: Technological innovations, enhanced performance, and future directions. *Results in Engineering*, 24(4):103521, 12 2024. ISSN 25901230. doi: 10.1016/j.rineng.2024.103521. URL https://doi.org/10.1007/s10901-017-9588-8.

[18] Keisuke Himoto. Conceptual framework for quantifying fire resilience – A new perspective on fire safety performance of buildings. *Fire Safety Journal*, 120, 3 2021. ISSN 0379-7112. doi: 10.1016/J.FIRESAF.2020.103052. URL https://www.sciencedirect.com/science/article/pii/S0379711220301090?casa_token=nr6F5PS77vsAAAAA:cizEmfIALTIoBg1ZyJvg8YWZW8-931M5p50I5tTtea4-x68Lt-JHYjLsUVXJuiyAUNVCQQkU_Q.

[19] Knauf Group. Fireboard 25mm, 2026. URL https://knauf.com/en-GB/p/product/fireboard-25mm-10085_0306.

[20] Dionysios I. Kolaitis, Eleni K. Asimakopoulou, and Maria A. Founti. Fire protection of light and massive timber elements using gypsum plasterboards and wood based panels: A large-scale compartment fire test. *Construction and Building Materials*, 73:163–170, 12 2014. ISSN 0950-0618. doi: 10.1016/J.CONBUILDMAT.2014.09.027. URL https://www.sciencedirect.com/science/article/pii/S0950061814010435?casa_token=tQojSbREoZcAAAAA:ZK87uJeuSf4NaP1gRlM3cfXHoemWYo4c6SwkqqDWBPS2ZGxuoGA_wUl2MoeA-Q-J3Yo_5768sA.

[21] Koninklijk Nederlands Normalisatie-instituut. NEN-EN 1991-1-2+C1+C2+C3/NB: Eurocode 1: Belastingen op constructies - Deel 1-2: Algemene belastingen - Belasting bij brand. 12 2018.

[22] R.M.M. van Liempd, H.L. de Witte, M. Karemaker, R.A.P. van Herpen, and V.D. Jansen. NIPV Rookverspreiding en persoonlijke veiligheid - Voorzieningen voor vluchtveiligheid en stay-in-place. 7 2022. URL https://nipv.nl/wp-content/uploads/2022/07/20220701-NIPV-Rookverspreiding-en-persoonlijke-veiligheid.pdf.

[23] Julie Liu and Erica C. Fischer. Review of large-scale CLT compartment fire tests. *Construction and Building Materials*, 318, 2 2022. ISSN 09500618. doi: 10.1016/J.CONBUILDMAT.2021.126099.

[24] Fredrik Ljunggren, Maria Fredriksson, Nils Johansson, and Angela Sasic Kalagasidis. Cross-laminated timber: a state-of-the-art review of moisture, fire, acoustics, and energy-related aspects. *Wood Material Science & Engineering*, 5 2025. ISSN 17480280. doi: 10.1080/17480272.2025.2507145. URL https://www.tandfonline.com/doi/pdf/10.1080/17480272.2025.2507145.

[25] Laura Lowden and Terence Hull. Flammability behaviour of wood and a review of the methods for its reduction. *Fire Science Reviews*, 2(1):4, 2013. ISSN 2193-0414. doi: 10.1186/2193-0414-2-4.

[26] Arthur. Lyons. *Materials for architects and builders*. Routledge, Taylor & Francis Group, sixth edition, 2020. ISBN 9780815363392.

[27] Cameron E. MacLeod, Angus Law, and Rory M. Hadden. Quantifying the heat release from char oxidation in timber. *Fire Safety Journal*, 138, 7 2023. ISSN 03797112. doi: 10.1016/J.FIRESAF.2023.103793.

[28] Cameron James McGregor. CONTRIBUTION OF CROSS LAMINATED TIMBER PANELS TO ROOM FIRES. Technical report, 1 2013.

[29] Robert McNamee, Jochen Zehfuss, Alastair I. Bartlett, Mohammad Heidari, Fabienne Robert, and Luke A. Bisby. Enclosure fire dynamics with a cross-laminated timber ceiling. *Fire and Materials*, 45(7):847–857, 11 2021. ISSN 10991018. doi: 10.1002/fam.2904. URL /doi/pdf/10.1002/fam.2904https://onlinelibrary.wiley.com/doi/abs/10.1002/fam.2904https://onlinelibrary.wiley.com/doi/10.1002/fam.2904.

[30] Alejandro R Medina Hevia. Fire Resistance of Partially Protected Cross-Laminated Timber Rooms. 2014. doi: 10.22215/ETD/2015-10728. URL https://hdl.handle.net/20.500.14718/32118.

[31] Ministerie van Binnenlandse Zaken en Koninkrijksrelaties. Artikel 4.17. Tijdsduur niet-bezwijken, 12 2025. URL https://wetten.overheid.nl/BWBR0041297/2025-07-01#Hoofdstuk4_Afdeling4.2_Paragraaf4.2.2_Artikel4.17.

[32] Ministerie van Binnenlandse Zaken en Koninkrijksrelaties. § 4.2.12. Hulpverlening bij brand, 7 2025. URL https://wetten.overheid.nl/BWBR0041297/2025-07-01#Hoofdstuk4_Afdeling4.2_Paragraaf4.2.12.

[33] Ministerie van Binnenlandse Zaken en Koninkrijksrelaties. § 4.2.2. Constructieve veiligheid bij brand, 7 2025. URL https://wetten.overheid.nl/BWBR0041297/2025-07-01#Hoofdstuk4_Afdeling4.2_Paragraaf4.2.2.

[34] Ministerie van Binnenlandse Zaken en Koninkrijksrelaties. § 4.2.8. Beperking van uitbreiding van brand, 7 2025. URL https://wetten.overheid.nl/BWBR0041297/2025-07-01#Hoofdstuk4_Afdeling4.2_Paragraaf4.2.8.

[35] Ministerie van Binnenlandse Zaken en Koninkrijksrelaties. § 4.2.7. Beperking van het ontwikkelen van brand en rook, 7 2025. URL https://wetten.overheid.nl/BWBR0041297/2025-07-01#Hoofdstuk4_Afdeling4.2_Paragraaf4.2.7.

[36] Ministerie van Binnenlandse Zaken en Koninkrijksrelaties. § 4.2.6. Beperking van het ontstaan van een brandgevaarlijke situatie, 7 2025. URL https://wetten.overheid.nl/BWBR0041297/2025-07-01#Hoofdstuk4_Afdeling4.2_Paragraaf4.2.6.

[37] Nederlands Normalisatie-Instituut. NEN 6055:2009 Fysisch brandmodel op basis van een natuurlijk brandconcept. 10 2009.

[38] Carl Pettersson. Fire Safety in Timber Buildings-A review of existing knowledge. Technical report, Brandforsk, 11 2023. URL www.redfireengineers.se.

[39] Sella van Poppel. Brandgedrag van kruislaaghout onder invloed van warmtestraling. 9 2023.

[40] Mary Schons. The Chicago Fire of 1871 and the 'Great Rebuilding', 10 2023. URL https://education.nationalgeographic.org/resource/chicago-fire-1871-and-great-rebuilding/.

[41] Ian Smith and Monica A. Snow. Timber: An ancient construction material with a bright future. *Forestry Chronicle*, 84(4):504–510, 2008. ISSN 00157546. doi: 10.5558/TFC84504-4. URL /doi/pdf/10.5558/tfc84504-4?download=true.

[42] Furkan Fatih Sönmez, Hesan Ziar, Olindo Isabella, and Miro Zeman. Fast and accurate ray-casting-based view factor estimation method for complex geometries. *Solar Energy Materials and Solar Cells*, 200, 9 2019. ISSN 09270248. doi: 10.1016/j.solmat.2019.109934.

[43] Péter Szabó, Petr Dobrovolný, Tomáš Kolář, Michal Rybníček, Josef Kyncl, and Tomáš Kyncl. Local timber dominated pre-industrial construction: Insights from archival and dendrochronological data. *Dendrochronologia*, 91:126337, 6 2025. ISSN 1125-7865. doi: 10.1016/J.DENDRO.2025.126337. URL https://www.sciencedirect.com/science/article/pii/S1125786525000517.

[44] R.A.P. van Herpen. Is woningbouw in CLT 'fire resilient'? 6 2021. URL https://www.brandveilig.com/artikel/is-woningbouw-in-clt-fire-resilient-68863.

[45] R.A.P. van Herpen. PHBO Fire Safety Engineering 1. Technical report, Arnhem, 2022.

[46] Gabri van Tussenbroek. Dendrochronological Research in Amsterdam Monuments: House Building, Timber Trade, and Methodological Implications. *International Journal of Wood Culture*, 3(1-3):9–25, 5 2023. ISSN 2772-3186. doi: 10.1163/27723194-BJA10012. URL https://www.sciencedirect.com/org/science/article/pii/S2772318623000206.

[47] Nick Voogt and Ralph Hamerlinck. Stappenplan voor FSE volgens de Nationale Bijlage bij NEN-EN 1991-1-2. URL https://www.brandveiligmetstaal.nl/pag/316/pagina.html.

[48] Merel Vos, Bahar Yildiz, Gustaf Jackson, and Joost van den Berg. CROSS TIMBER LAMINATED HANDLEIDING VOOR ARCHITECTEN. 2 2021. URL https://inbo.com/wp-content/uploads/2022/12/CLT-Handleiding-voor-architecten-en-bouwkundigen.pdf.

[49] Felix Wiesner, Luke A. Bisby, Alastair I. Bartlett, Juan P. Hidalgo, Simón Santamaria, Susan Deeny, and Rory M. Hadden. Structural capacity in fire of laminated timber elements in compartments with exposed timber surfaces. *Engineering Structures*, 179:284–295, 1 2019. ISSN 18737323. doi: 10.1016/J.ENGSTRUCT.2018.10.084.

[50] Qi Ye, Yingchun Gong, Haiqing Ren, Lin Peng, and Houjiang Zhang. Theoretical, numerical and experimental studies on thermal insulation performance of different cross laminated timber walls. *Journal of Building Engineering*, 72:106640, 8 2023. ISSN 2352-7102. doi: 10.1016/J.JOBE.2023.106640. URL https://www.sciencedirect.com/science/article/pii/S2352710223008197.

[51] Adel Younis and Ambrose Dodoo. Cross-laminated timber for building construction: A life-cycle-assessment overview. *Journal of Building Engineering*, 52:104482, 7 2022. ISSN 2352-7102. doi: 10.1016/J.JOBE.2022.104482. URL https://www.sciencedirect.com/science/article/pii/S2352710222004958.

[52] Annarita Zarrillo. The History of Wood in Constructions Between Past and Present. *Modern Environmental Science and Engineering*, 5(11):1027–1032, 11 2019. ISSN 23332581. doi: 10.15341/mese(2333-2581)/11.05.2019/006.

[53] J. Zehfuss and D. Hosser. A parametric natural fire model for the structural fire design of multi-storey buildings. *Fire Safety Journal*, 42(2):115–126, 3 2007. ISSN 0379-7112. doi: 10.1016/J.FIRESAF.2006.08.004. URL https://www.sciencedirect.com/science/article/abs/pii/S0379711206000993.

[54] Yongwang Zhang, Xiaofei Zhang, and Lu Wang. Experimental validation and simplified design of an energy-based time equivalent method applied to evaluate the fire resistance of the glulam exposed to parametric fire. *Engineering Structures*, 272, 12 2022. ISSN 0141-0296. doi: 10.1016/J.ENGSTRUCT.2022.115051. URL https://www.sciencedirect.com/science/article/pii/S0141029622011270.

Appendices

A View Factor Calculation

$$f_A = \frac{\frac{b_1}{d}}{\sqrt{1+\frac{b_1}{d}^2}} \cdot \arctan(\frac{\frac{h_1}{d}}{\sqrt{1+\frac{b_1}{d}^2}} + \frac{\frac{h_1}{d}}{\sqrt{1+\frac{h_1}{d}^2}}) \cdot \arctan(\frac{\frac{b_1}{d}}{\sqrt{1+\frac{h_1}{d}^2}})$$

$$f_B = \frac{\frac{b_2}{d}}{\sqrt{1+\frac{b_2}{d}^2}} \cdot \arctan(\frac{\frac{h_1}{d}}{\sqrt{1+\frac{b_2}{d}^2}} + \frac{\frac{h_1}{d}}{\sqrt{1+\frac{h_1}{d}^2}}) \cdot \arctan(\frac{\frac{b_2}{d}}{\sqrt{1+\frac{h_1}{d}^2}})$$

$$f_C = \frac{\frac{b_1}{d}}{\sqrt{1+\frac{b_1}{d}^2}} \cdot \arctan(\frac{\frac{h_2}{d}}{\sqrt{1+\frac{b_1}{d}^2}} + \frac{\frac{h_2}{d}}{\sqrt{1+\frac{h_2}{d}^2}}) \cdot \arctan(\frac{\frac{b_1}{d}}{\sqrt{1+\frac{h_2}{d}^2}})$$

$$f_D = \frac{\frac{b_2}{d}}{\sqrt{1+\frac{b_2}{d}^2}} \cdot \arctan(\frac{\frac{h_2}{d}}{\sqrt{1+\frac{b_2}{d}^2}} + \frac{\frac{h_2}{d}}{\sqrt{1+\frac{h_2}{d}^2}}) \cdot \arctan(\frac{\frac{b_2}{d}}{\sqrt{1+\frac{h_2}{d}^2}})$$

$$f_{tot} = f_A + f_B + f_C + f_D$$

B Rate of Heat Release Graphs

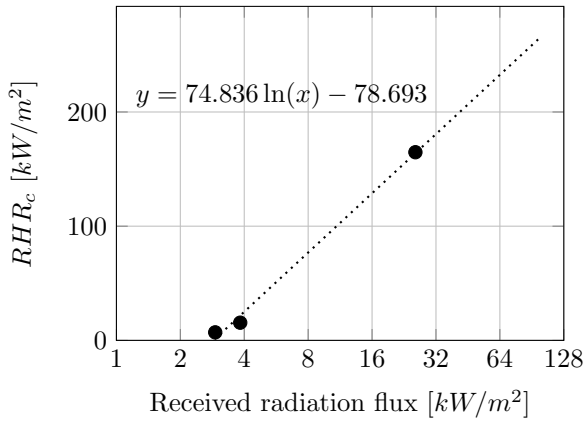

(a) CLT fully exposed

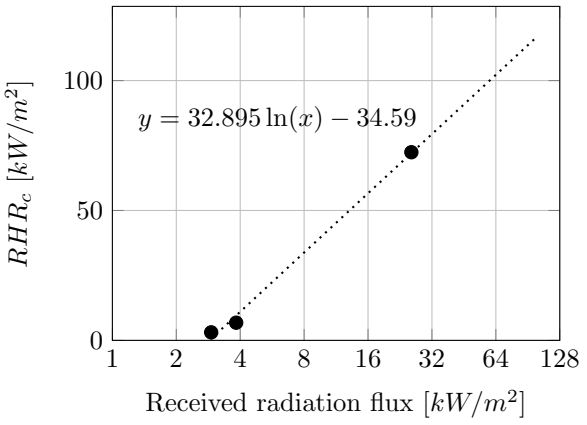

(b) CLT ceiling exposed only

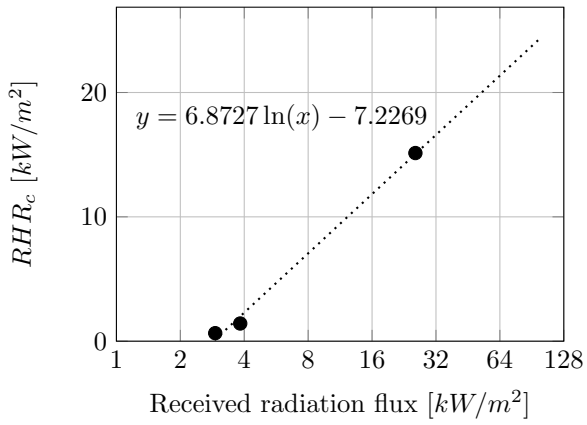

(c) CLT one wall exposed

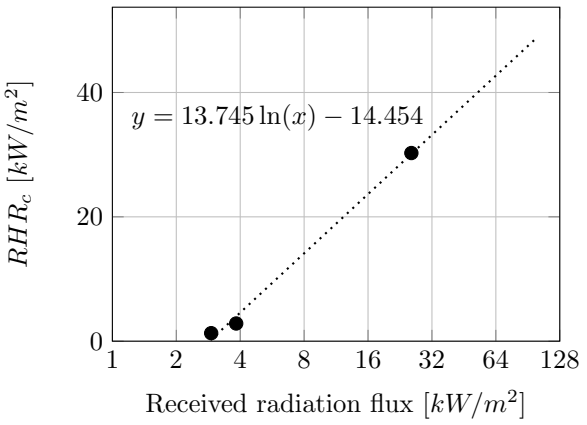

(d) CLT two walls exposed

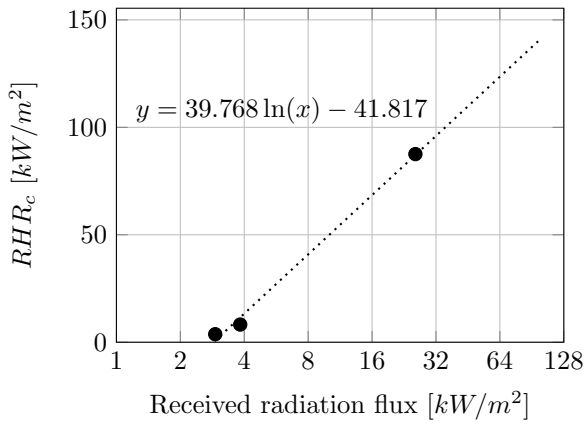

(e) CLT ceiling and one wall exposed

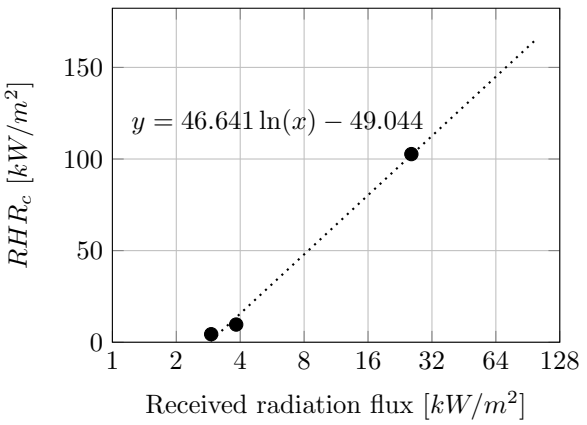

(f) CLT ceiling and two walls exposed

Figure 7: Comparison of measured data and trends for different exposure configurations

C OZone Report Baseline Model

Header

OZone V 3.0.4 Report

ANALYSIS

Analysis Name:

File Name:C:\Users\20223284\OneDrive - TU Eindhoven\Desktop\OZone\cltfullycovered.ozn

Created: 09/02/2026 at 14:46:13

Strategy

Select Analysis Strategy: Combination (default)

Transition (2 Zones to 1 Zone) Criteria

Upper Layer Temperature ≥ 500 °C

Combustible in Upper Layer + U.L. Temperature ≥ Combustible Ignition Temperature = 300 °C

Interface Height ≤ 0.2 x Compartment Height

Fire Area ≥ 0.25 x Floor Area

Parameters

Openings

Radiation Through Closed Openings: 0.8

Bernoulli Coefficient: 0.7

Physical Characteristics of Compartment

Initial Temperature: 293 K

Initial Pressure: 100000 Pa

Parameters of Wall Material

Convection Coefficient at the Hot Surface: 25 W/m²K

Convection Coefficient at the Cold Surface: 9 W/m²K

Calculation Parameters

End of Calculation: 14400 sec

Time Step for Printing Results: 60 sec

Maximum Time Step for Calculation: 10 sec

Air Entrained Model:Heskestad

Temperature Dependent Openings

Temperature Dependent: 400 °C

Stepwise Variation

Temperature	% of Total Openings
[°C]	[%]
20	10
400	50
500	100

Linear Variation

Temperature	% of Total Openings
[°C]	[%]
20	10
400	50
500	100

Time Dependent Openings

Time	% of Total Openings
[sec]	[%]
0	5
1200	100

Compartment...

Compartment Geometry: Rectangular Floor

Height: 3 m

Depth: 7 m

Length: 10 m

Flat Roof

Floor

Material	Thickness	Unit mass	Conductivity	Specific Heat	Rel Emissivity	Rel Emissivity
	[cm]	[kg/m³]	[W/mK]	[J/kgK]	Hot Surface	Rel Emissivity
Normal weight Concrete [EN1994-1-2]	10	2300	1.6	1000	0.8	0.8

Normal Wood	16	450	0.1	1113	0.8	0.8

Ceiling

Material	Thickness	Unit mass	Conductivity	Specific Heat	Rel Emissivity	Rel Emissivity
	[cm]	[kg/m³]	[W/mK]	[J/kgK]	Hot Surface	Rel Emissivity
Gypsum board [EN12524]	2.5	900	0.25	1000	0.8	0.8
Normal Wood	16	450	0.1	1113	0.8	0.8
Normal weight Concrete [EN1994-1-2]	10	2300	1.6	1000	0.8	0.8

Wall 1

Material	Thickness	Unit mass	Conductivity	Specific Heat	Rel Emissivity	Rel Emissivity
	[cm]	[kg/m³]	[W/mK]	[J/kgK]	Hot Surface	Rel Emissivity
Gypsum board [EN12524]	2.5	900	0.25	1000	0.8	0.8
Normal Wood	11	450	0.1	1113	0.8	0.8

Openings

Sill Height Hi	Soffit Height Hs	Width	Variation	Adiabatic
[m]	[m]	[m]		
0.5	2	4.25	Constant	no

Wall 2

Material	Thickness	Unit mass	Conductivity	Specific Heat	Rel Emissivity	Rel Emissivity
	[cm]	[kg/m³]	[W/mK]	[J/kgK]	Hot Surface	Rel Emissivity
Gypsum board [EN12524]	2.5	900	0.25	1000	0.8	0.8
Normal Wood	11	450	0.1	1113	0.8	0.8

Wall 3

Material	Thickness	Unit mass	Conductivity	Specific Heat	Rel Emissivity	Rel Emissivity
	[cm]	[kg/m³]	[W/mK]	[J/kgK]	Hot Surface	Rel Emissivity
Gypsum board [EN12524]	2.5	900	0.25	1000	0.8	0.8
Normal Wood	11	450	0.1	1113	0.8	0.8

Openings

Sill Height Hi	Soffit Height Hs	Width	Variation	Adiabatic
[m]	[m]	[m]		
0.5	2	4.25	Constant	no

Wall 4

Material	Thickness	Unit mass	Conductivity	Specific Heat	Rel Emissivity	Rel Emissivity
	[cm]	[kg/m³]	[W/mK]	[J/kgK]	Hot Surface	Rel Emissivity
Gypsum board [EN12524]	2.5	900	0.25	1000	0.8	0.8
Normal Wood	11	450	0.1	1113	0.8	0.8

Fire...

Compartment Fire:: Annex E (EN 1991-1-2)

Max Fire Area: 70 m^2

Fire Elevation: 1 m

Fuel Height: 3 m

Occupancy	Fire Growth Rate	RHRf	Fire Load qf,k	Danger of Fire Activation
		[kW/m²]	80% Fractile [MJ/m²]	
User Defined	300	250	870	1

Active Fire Fighting Measures

Automatic Water Extinguishing System		δ_1=1
Independent Water Supplies		δ_2=1
Automatic Fire Detection by Heat		$\delta_{3,4}$=1
Automatic Fire Detection by Smoke		
Automatic Alarm Transmission to Fire Brigade		δ_5=1
Work Fire Brigade		$\delta_{6,7}$=1
Off Site Fire Brigade		
Safe Access Routes	on	δ_8=1
Staircases Under Overpressure in Fire Alarm		
Fire Fighting Devices	on	δ_9=1
Smoke Exhaust System	on	δ_{10}=1

Fire Risk Area: 12.5 m^2 $\delta_{q,1}$ = 1

Danger of Fire Activation:$\delta_{q,2}$ = 1

Active Measures:$\Pi\delta_{n,i}$ = 1

$q_{f,d}$ = 696.0

Combustion Heat of Fuel: 17.5MJ/kg

Combustion Efficiency Factor: 0.8

Combustion Model:External flaming

RESULTS

Fire Area: The maximum fire area (70.00m²) is greater than 25% of the floor area (70.00m²). The fire load is uniformly distributed.

Switch to one zone + Fully engulfed fire: Temperature of zone in contact with fuel >300.0°C at time [s] 497.24

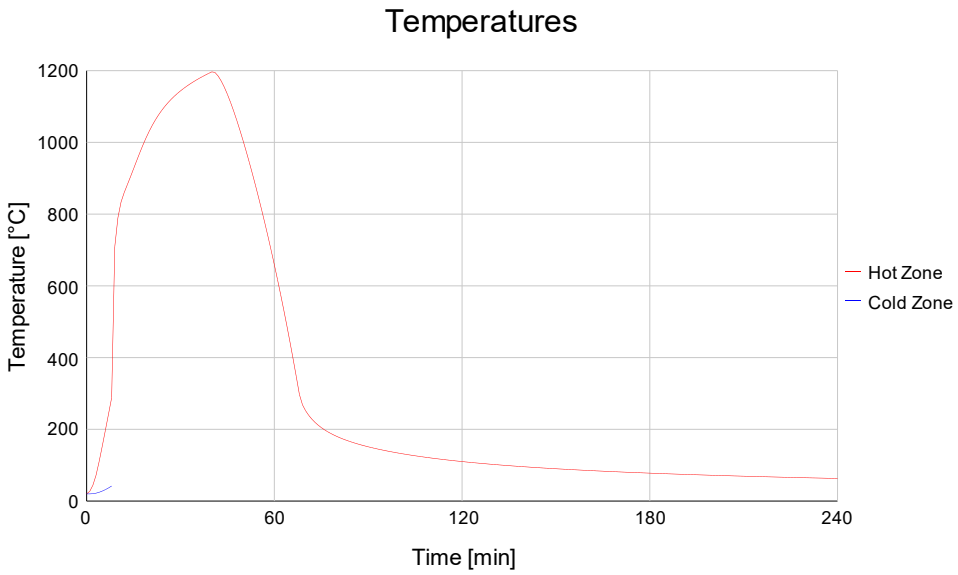

Figure 1. Hot and Cold Zone Temperature

Max: 1197°C At:40 min

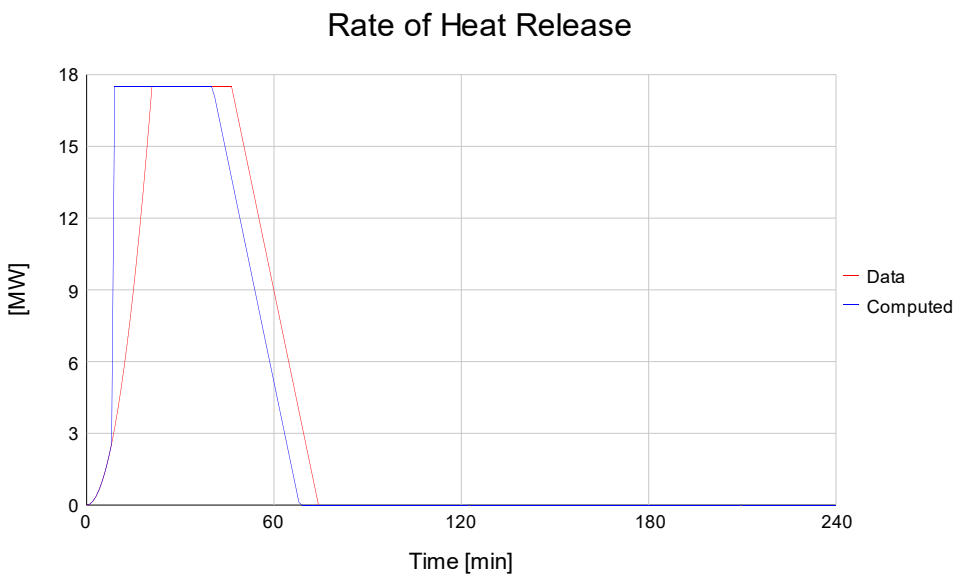

Figure 2. RHR Data and Computed

Max: 17.50MW At:20.9 min

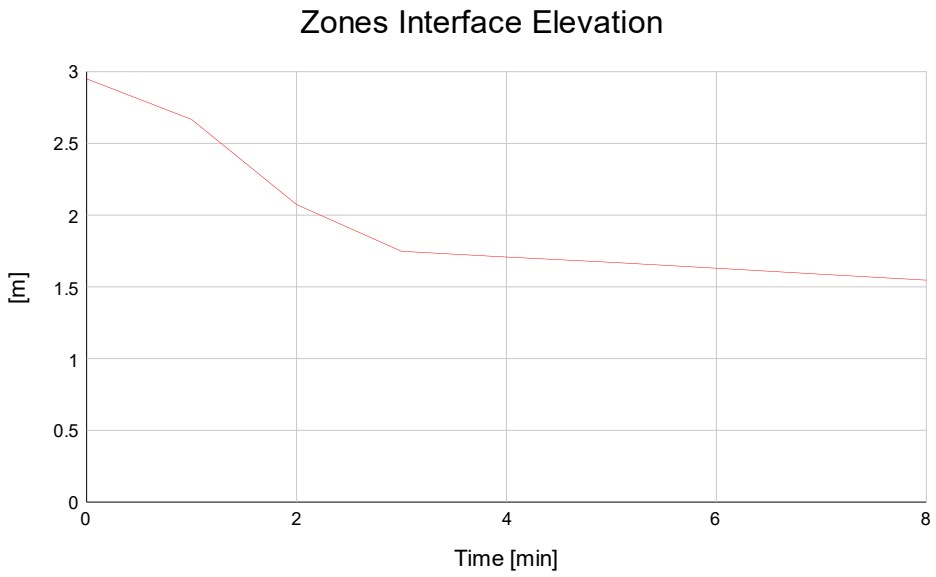

Figure 4. Zones Interface Elevation

Max: 1.55m At:8.00 min

Steel Profile...

Cross Section: Unprotected Cross Section

Steel Profile: IPE AA 80

Exposure: Exposed on Four Sides

Heating...

Profile Heated By: Hot Zone Temperature